AEROSOL FLOW RESISTANCE
IN HORIZONTAL CAPILLARY TUBING

A THESIS

Presented to

the Faculty of the Graduate Division

Georgia Institute of Technology

In Partial Fulfillment

of the Requirements for the Degree

Master of Science in Chemical Engineering

By

Robert Gordon Wooten

December 1955

"In presenting the dissertation as a partial fulfillment of the requirements for an advanced degree from the Georgia Institute of Technology, I agree that the Library of the Institution shall make it available for inspection and circulation in accordance with its regulations governing materials of this type. I agree that permission to copy from, or to publish from, this dissertation may be granted by the professor under whose direction it was written, or such copying or publication is solely for scholarly purposes and does not involve potential financial gain. It is understood that any copying from, or publication of, this dissertation which involves potential financial gain will not be allowed without written permission.

_____

_____"

6 N
12 R

AEROSOL FLOW RESISTANCE
IN HORIZONTAL CAPILLARY TUBING

Approved:

Thesis Adviser

Date Approved by Chairman: December 16, 1955

ACKNOWLEDGEMENTS

The author wishes to express his sincere appreciation to Professor Joseph M. DallaValle, not only for his suggestion of this problem and his guidance throughout the work, but for his constant optimistic attitude which was invaluable in the prosecution of this thesis project. The author would like to express his thanks to the School of Chemical Engineering of Georgia Institute of Technology for assistance in obtaining necessary equipment, to the Haloid Company of Rochester, New York, for providing the cloud generator and the fine carbon powder, and to the Superior Tube Company of Norristown, Pennsylvania, for their kind gift of the small diameter nickel tubing. The author also would like to express appreciation to his wife for her constant encouragement and careful typing.

SYMBOLS

Symbol	Definition	English Units
A_p	Cross-sectional Area of Particle	ft^2
A_t	Cross-sectional Area of Tube	ft^2
a	Acceleration	ft/sec^2
C_D	Over-all Drag Coefficient	Dimensionless
D_t	Inside Diameter of Tube	ft
d	Differential Operator	—
d_p	Particle Diameter	ft
d_w	Weight-average Particle Diameter	ft
F_d	Drag or Resistance to Motion	lb-force
f_A	Alves Friction Factor	Dimensionless
f_a	Fanning Friction Factor	Dimensionless
f_C	Culgan Friction Factor	Dimensionless
f_p	Particle Friction Factor	Dimensionless
G	Average Particle Diameter by Count	ft
G_a	Mass Rate of Flow of Air	$\frac{\text{lb-mass}}{\text{ft}\cdot\text{ft}\cdot\text{sec}}$
G_{mean}	Mass Rate of Flow of Mixture	"
G_p	Mass Rate of Flow of Solids	"
g	Acceleration of Gravity	ft/sec^2
g_c	Newton Law Conversion Factor	$\frac{\text{lb-mass}\cdot\text{ft}}{\text{lb-force}\cdot\text{sec}^2}$
h_m	Head Loss (in terms of air)	ft
k	Constant	Dimensionless
L	Tube Length	ft
ΔL	Tube Length (Pressure drop across)	ft
M	Molecular Weight	$\frac{\text{lb-mass}}{\text{lb-mole}}$
m_p	Mass of Particle	lb-mass
N	Number of Particles	Dimensionless
P	Absolute Pressure	$lb\text{-force}/ft^2$
P_1	Absolute Pressure in Manifold No.1	$lb\text{-force}/ft^2$
P_2	Absolute Pressure in Manifold No.2	$lb\text{-force}/ft^2$
P_s	Partial Pressure of Water	$lb\text{-force}/ft^2$
ΔP	Pressure Drop across ΔL	$lb\text{-force}/ft^2$
ΔP_{sub}	(Subscripts defined below)	$lb\text{-force}/ft^2$
Q_a	Volume Flow Rate of Air	ft^3/sec
R_o	Gas Constant	$\frac{\text{ft}\cdot\text{lb-force}}{\text{lb-mole}\cdot{}^\circ R}$
R	Specific Loading $\equiv W_p/W_a$	Dimensionless
$(Re)_a$	Air Reynolds Number	Dimensionless
$(Re)_p$	Particle Reynolds No. $\equiv d_p \rho_a (u_a - u_p)/\mu$	Dimensionless

Symbol	Definition	English Units
$(Re)_m$	Mean Reynolds Number $\equiv D_t G_a (1+R)/\mu$	Dimensionless
T	Absolute Temperature	^oR
t	Time	sec
u_a	Air Velocity	ft/sec
u_p	Particle Velocity	ft/sec
u_r	Relative or Slip Velocity	ft/sec
u_{ff}	Free Fall Velocity of Particle	ft/sec
W_a	Weight Rate of Flow of Air	lb-mass/sec
W_p	Weight Rate of Flow of Solids	lb-mass/sec
α	Pressure Drop Ratio $\equiv \Delta P_{ft}/\Delta P_{fa}$	Dimensionless
β	Functional Relation	—
Δ	Finite Difference Operator	—
μ	Dynamic Viscosity of Air	lb-mass/ft·sec
ρ_a	Density of Air	lb-mass/ft^3
ρ_{ds}	Density of Dispersed Phase $\equiv W_p u_a/Q_a u_p$	lb-mass/ft^3
ρ_m	Mean Density of Phases $\equiv \rho_a+\rho_{ds}$	lb-mass/ft^3
ρ_p	Density of Particle	lb-mass/ft^3
σ_g	Geometric Standard Deviation	Dimensionless
Φ	Functional Relation	—

Subscript	Definition
A	Alves, George E. in Lapple, Alves, et al (14)
a	Air
C	Culgan, J. M. in Culgan (5)
p	Particle
r	Relative
aa	Acceleration, Air
ap	Acceleration, Particle
ds	Dispersed Phase
fa	Friction, Air
fp	Friction, Particle
ft	Friction, Total
m	Mean (Usually arithmetical)
sa	Static, Air
sp	Static, Particle
T	Total
t	Tube
w	Weight-average
1	Manifold No. 1
2	Manifold No. 2
3	Wet Test Meter

Superscript	Definition
*	Equilibrium Condition

TABLE OF CONTENTS

(Continued)

TABLE OF CONTENTS (Concluded)

LIST OF FIGURES

LIST OF TABLES

CHAPTER I

SUMMARY

The purpose of this thesis is to investigate the resistance to flow of a solid-air suspension through very small diameter tubing. Though considerable work on the two-phase flow of solid-air suspensions has been reported, the solid particles have always been larger then ten microns in diameter. This thesis considers the case of carbon particles, approximately one micron in diameter, carried in an air stream through a capillary tube.

Equipment is assembled so that these aerosols may, by pressure differential, be caused to flow through horizontal capillary tubing. These capillary tubes have internal diameters of 0.0199, 0.0379, 0.0521, and 0.0808 inch. The equipment is constructed so that pressures, temperatures, and flow rates may be measured.

Data are obtained by measuring the pressure drop accompanying the flow of various suspensions at different air rates and solids concentrations. The mass air rates vary from one to twenty pounds per second per square foot, while the solids concentrations vary from 5×10^{-4} to 1.6×10^{-2} pounds solids per pound of air.

The equations, which have been proposed in the literature for solid-air suspension flow, are used in an effort to correlate the experimental data of this thesis. The equation proposed by Alves (14) most successfully represents the data.

$$\Delta P_{ft} = \left(\frac{4f_A \Delta L}{D_t}\right)\left(\frac{G_a^2}{2g_c}\right)(1+R)\left(\frac{1}{\rho_a}+\frac{R}{\rho_p}\right)$$

When f_A is plotted versus a modified Reynolds number,

$$(Re)_m = \frac{D_t G_a}{\mu}(1+R)$$

the familiar Fanning type lines for the streamline, intermediate, and turbulent regions are formed.

However, the values of f_A are higher than the corresponding Fanning friction factors, f_a. Therefore, this equation is not recommended for design purposes until more data covering a wider range of variables are presented and the values of f_A verified.

It is shown indirectly that the slip velocity, u_r, is very small or negligible. This is evident from the success of the Alves equation, which is a modified Fanning equation. The aerosol appears to behave very much like a true fluid.

CHAPTER II

INTRODUCTION

Literature review. — No work is reported in the literature on aerosol flow resistance in capillary tubing. However, considerable work is reported on the flow of solid-air systems through pipes, where the solid particles as well as the pipes are much larger than those in this thesis project. These workers propose correlations for such systems based on both theoretical and empirical considerations. Though certain differences are expected, such work has a direct bearing on aerosol flow and thus will be briefly reviewed in this chapter.

One of the first to look into this matter of pressure drops with solid-air suspension flow is Gasterstadt (9). Gasterstadt, using suspensions of wheat in air, concludes from his data, that α, the ratio of the total pressure drop to the air pressure drop, plotted versus R, the specific loading, should yield a straight line for any one air velocity. Thus:

$$\alpha = 1 + kR \qquad (1)$$

Vogt and White (19) report that Segler (17), using another

air-wheat system, confirms the findings of Gasterstadt.

Farbar (8), in a much more recent article, finds that α versus R gives a line, which is straight for high values of R, but tends to curve into the (0,1) point. Though Farbar plots the points for two different air rates in showing this, he admits that several lines might be drawn for the different air rates. Farbar's work is based on findings from systems of alumina, silica, and catalyst in air flowing in both horizontal and vertical glass test sections 17 mm. in inside diameter. The sizes of the particles vary from 10 microns to 220 microns, air velocities from 50 to 150 feet per second, and values of R from 0 to 16 pounds of solid per pound of air. Farbar also plots total pressure drop versus air rate and for each value of R gets essentially parallel straight lines in this linear plot.

Vogt and White (19) obtain data on the flow of suspensions of sand, steel shot, clover seed, and wheat in air through a half-inch standard iron pipe. These data and the data of Gasterstadt (9) and Segler (17) are used as a basis for proposing an equation for both horizontal and vertical flow:

$$\alpha - 1 = A\left(\frac{D_t}{d_p}\right)^2\left(\frac{\rho_a}{\rho_p} \times \frac{R}{(Re)_a}\right)^k \qquad (2)$$

where A and k are empirical functions of:

$$\sqrt{\frac{1/3(\rho_p-\rho_a)\rho_a g_c d_p^3}{\mu}} \qquad (3)$$

Vogt and White plot α-1/R versus $(Re)_a(d_p/D_t)^2(\rho_p/\rho_a)$ on a log-log grid and find that a straight line represents most of their data. Also these workers find that a plot of α-1 versus $(d_p/D_t)^2[\rho_p(Re)_a/\rho_a R]^k$ on a log-log grid gives a series of straight lines, one line for each material.

Belden and Kassel (2) present pressure drop data for the vertical transport of catalyst, approximately 0.04 and 0.08 inch in diameter, in pipes of approximately one inch and a half inch in diameter. On the basis of their data, they point out that Vogt and White (19) have apparently placed an incorrect dependence on the ratio of tube diameter to particle diameter. They propose that:

$$\frac{dP_{ft}}{dL} = \frac{2f_a(G_a+G_p)u_a}{g_c D_t} \qquad (4)$$

and show a correlation on a linear plot of:

$$f_a(Re)_a^{0.2} \text{ versus } \frac{G_a G_p}{(G_a+G_p)^2} \qquad (5)$$

Though the points are observed to be very scattered, these

workers draw a straight line to represent the data. Also, Belden and Kassel take the data of Vogt and White (19) and plotting α-1 versus $(Re)_a G_a/G_p$ on a log-log grid find that the data are represented by a straight line.

Albright and co-workers (1) study pressure drops of mixtures of air and coal (90 per cent through 200 mesh) in horizontal tubes where R is between 141 and 256 pounds of coal per pound of air. Air rate varies between seven and thirty-two feet per second, which gives Reynolds numbers from 600 to 10,000. These investigators make a log-log plot of f_a versus mass velocity and find several curved lines, one for each tube diameter, if the value of R is held constant. Also, a log-log plot of α-1 versus $(Re)_a \rho_p/R\rho_a D_t$ gives a single curved line.

Alves in the book by Lapple, Alves,et al (14) states that the total pressure drop in solid-gas systems may be broken up into the following:

(a) ΔP_{aa} (Acceleration of the air)

(b) ΔP_{fa} (Air friction)

(c) $\Delta P_{ap}+\Delta P_{fp}$ (Accelerate and keep solids suspended)

(d) ΔP_{sa} (Support of air in vertical tubes)

(e) ΔP_{sp} (Support of solids in vertical tubes)

Alves proposes use of the equation:

$$\Delta P_{ft} = \left(\frac{4f_A \Delta L}{D_t}\right)\left(\frac{G_a^2}{2g_c}\right)(1+R)\left(\frac{1}{\rho_a} \quad \frac{R}{\rho_p}\right) \qquad (6)$$

and suggests:

$$(Re)_m = \frac{D_t G_a}{\mu}(1+R) \qquad (7)$$

In theory, f_A should be the familiar Fanning friction factor, f_a. However, Alves notes that the use of this method for design will result in calculated pressures somewhat lower than observed pressures.

Culgan (5) studies the flow of suspensions of materials of approximately unit specific gravity (i.e. soybeans, coarse Tenite, fine Tenite, cottonseed, and Alundum) in a three inch nominal diameter horizontal plastic pipe. The materials used range in average diameter from approximately 0.0165 to 0.261 inch. Air flow rates vary from 12 to 21 pounds per minute. He plots the friction factor defined in equation (8) versus $(Re)_m$ and obtains a stepwise series of points. Culgan's friction factor, f_C, is very similar to that of Alves (14) given in equation (6). Culgan used:

$$f = \frac{2g_c D_t h_m}{u_a^2 \Delta L} \qquad (8)$$

To obtain a better correlation for his data, Culgan proposes the equation:

$$f_C = \frac{2g_c D_t h_m}{u_a^2 \Delta L}\left(\frac{\rho_m}{\rho_p}\right)^{\mathbb{D}(\rho_p)} \qquad (9)$$

From his data, involving unit specific gravity materials, he finds that $\Phi(\rho_p) = 0.25$ gives a satisfactory correlation. He proposes further investigation to determine the true nature of the function, $\Phi(\rho_p)$. Culgan also investigates to some extent particle velocity, relative velocity, pipe wall roughness, and initial settling or slugging.

Hinkle (11), using solid-air systems flowing in two inch and three inch horizontal glass pipes, obtains pressure drops and by photographic means obtains particle velocities. The materials examined are polystyrene beads, Tenite pellets, Alundum catalyst supports, and Catalin spheres. These materials range from 0.014 to 0.33 inch in diameter. Hinkle does an excellent job working with particle velocity and his comparison of observed velocity with calculated velocity is satisfactory. However, his handling of pressure drop leaves much to be desired. Hinkle proposes breaking up the pressure and treating each part separately just as Lapple, Alves, et al (14) do. In considering the constant velocity section he gives:

$$\Delta P_T/\Delta L = \Delta P_{fa}/\Delta L + \Delta P_{fp}/\Delta L \qquad (10)$$

Then dividing equation (10) by $\Delta P_{fa}/\Delta L$ obtains:

$$\frac{\Delta P_{ft}/\Delta L}{\Delta P_{fa}/\Delta L} = 1 + \frac{\Delta P_{fp}/\Delta L}{\Delta P_{fa}/\Delta L} \qquad (11)$$

The equation of Fanning is given as:

$$\Delta P_{fa}/\Delta L = \frac{f_a u_a^2}{2 g_c D_t} \rho_a \qquad (12)$$

Hinkle then proposes an analogous equation for the solids:

$$\Delta P_{fp}/\Delta L = \frac{f_p u_p^{*2}}{2 g_c D_t} \rho_{ds} \qquad (13)$$

After algebraic substitutions, he derives the equation:

$$\alpha = \frac{\Delta P_{ft}/\Delta L}{\Delta P_{fa}/\Delta L} = 1 + \frac{f_p u_p^*}{f_a u_a} \cdot R \qquad (14)$$

Hinkle (11) then attempts to correlate his experimental data with equation (14). In his Sample Calculations (on p. 95) he states that the solids friction factor is obtained from the following equation:

$$f_p = \frac{2(\Delta P_{fp}/\Delta L) g_c D_t A_t}{u_p^* W_p} \qquad (15)$$

Regardless of what value of u_p^* is used, it is easily seen that Hinkle has obtained $f_p u_p^*$ from the equation:

$$f_p u_p^* = \frac{2(\Delta P_{fp}/\Delta L) g_c D_t A_t}{W_p} \qquad (16)$$

Thus, when Hinkle attempts to correlate data using equation (14), he is in reality substituting equation (16) and equation (12) into equation (14). This gives:

$$\alpha = \frac{\Delta P_{ft}/\Delta L}{\Delta P_{fa}/\Delta L} = 1 + \frac{2(\Delta P_{fp}/\Delta L) g_c D_t A_t}{W_p (\Delta P_{fa}/\Delta L) 2 g_c D_t \rho_a u_a} \cdot \frac{W_p}{W_a} \qquad (17)$$

Since continuity demands that $W_a/A_t = G_a = u_a \rho_a$, equation (17) reduces to:

$$\alpha = \frac{\Delta P_{ft}/\Delta L}{\Delta P_{fa}/\Delta L} = 1 + \frac{\Delta P_{fp}/\Delta L}{\Delta P_{fa}/\Delta L} \qquad (18)$$

When equation (18) is compared with equation (13), it is obvious that when Hinkle plots α versus $(f_p u_p^*/f_a u_a)R$, as he does on p. 65, he has simply plotted $\Delta P_{ft}/\Delta P_{fa}$ versus $(\Delta P_{ft}/\Delta P_{fa})-1$ or α versus $\alpha-1$. Such a plot will give a straight line regardless of the data. Thus, Hinkle has not given a reasonable correlation. This same criticism applies to Hinkle's attempted correlation of the data of Hariu and Molstad (10) given on p.69 of Hinkle's (11) thesis. One wonders also, how ΔP_T was calculated to make the plot in Hinkle's thesis (p. 71). An excellent contribution could have been made, had Hinkle attempted to relate

f_p with other factors, perhaps even $(Re)_p$.

Many authors such as Cramp (4), Jennings (12), Chatley (3), Korn (13), Wood and Bailey (21), and DallaValle (6) give excellent theoretical treatments of the problem of solid-air suspension flow. Such investigations point out the importance of the particle velocity in such systems. Work has been done investigating the particle velocity by many of the workers previously cited in references and also by Wagon (20), Upenskii (18), and Zenz (22). Though it appears that particle velocity is the key to the problem, u_p is unknown in this thesis and thus correlations not involving particle velocity must be used. For this reason, such correlations have been more fully discussed while those involving particle velocity have been only mentioned.

Objectives of investigation. — This thesis is a presentation of pressure drop data obtained when aerosols of various solids concentrations are caused to flow through horizontal capillary tubes. An attempt is made to correlate these data by means of equations proposed by the investigators in the above Literature Review. Though their correlations are based on particles much larger than the particles used in this investigation, it is to be expected that the data of this thesis may be correlated by some of these equations. Therefore, this thesis is mainly

an attempt to use previously proposed relations to represent the data. The success or failure of such relations to represent the data of this project is discussed in terms of particle size. No new equation is proposed in this thesis, because it is felt that more accurate data, covering a wider range of variables and including some particle velocity data, should be obtained before any equation is proposed. This thesis is a first attempt at understanding the flow resistance of aerosols in horizontal capillary tubing.

CHAPTER III

EXPERIMENTAL METHODS

Apparatus. — The experimental apparatus used in obtaining the data of this thesis is illustrated in Fig. 1 and Fig. 2. Fig. 1 is an ink drawing representing and labeling all of the essential components of the apparatus while Fig. 2 is a photographic representation of this equipment. The equipment in functioning must 1.) provide a constant pressure air supply; 2.) create a solid-air suspension; 3.) by pressure differential cause the suspension to flow through a capillary tube; 4.) measure the pressure and temperature of the suspension as it enters and as it leaves the capillary tube; and 5.) provide a means of separating the solid and air phases and measuring the flow rate of each. The components used to perform these functions are discussed below in the same order as the functions are listed above.

There are several methods of obtaining a constant pressure supply when the pressure of the available air source varies over a wide range. Two of the most economical methods are the Cartesian diver and the self-operated pressure regulator. A commercial model of the Cartesian

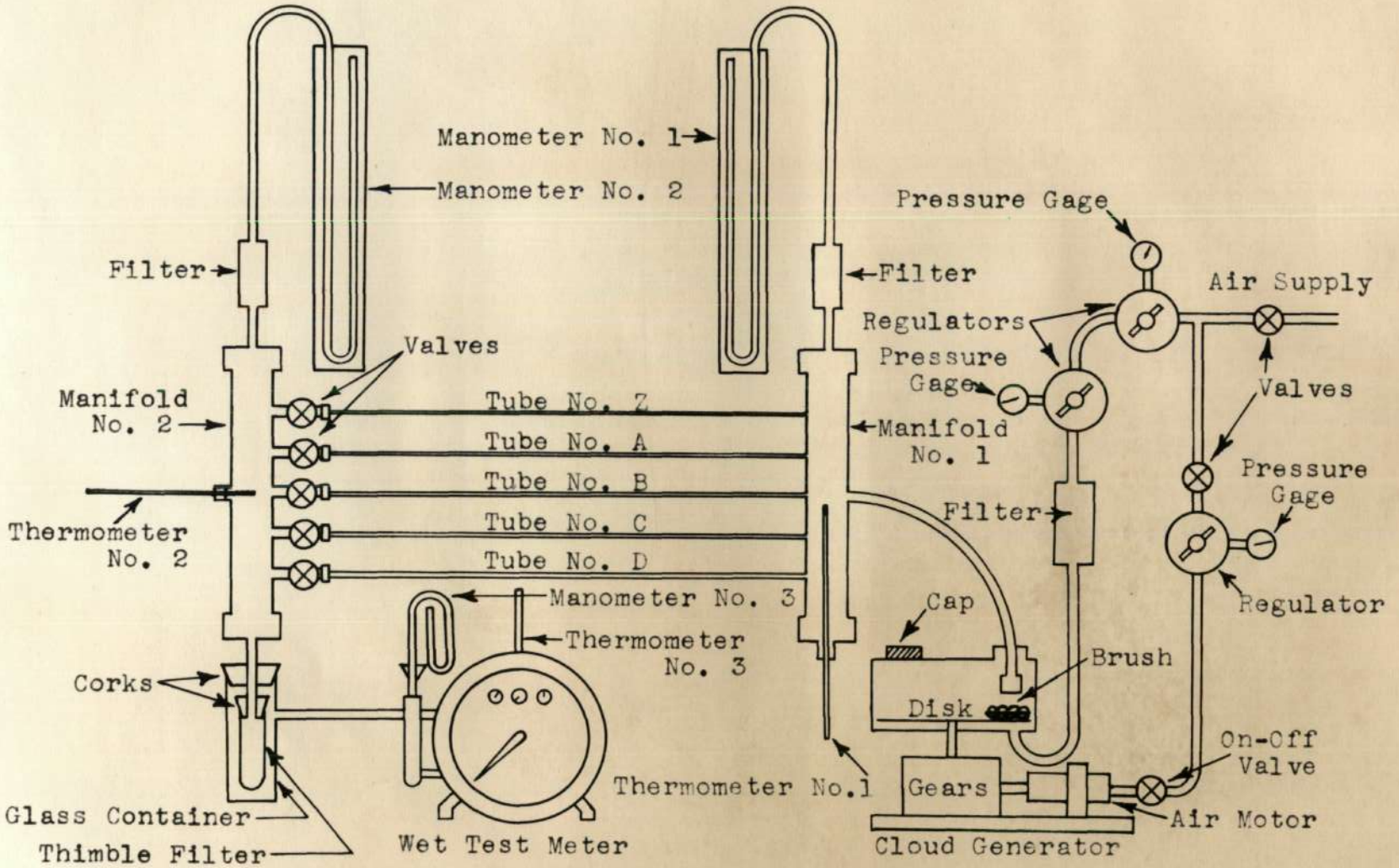

Fig. 1 Diagram of Experimental Apparatus

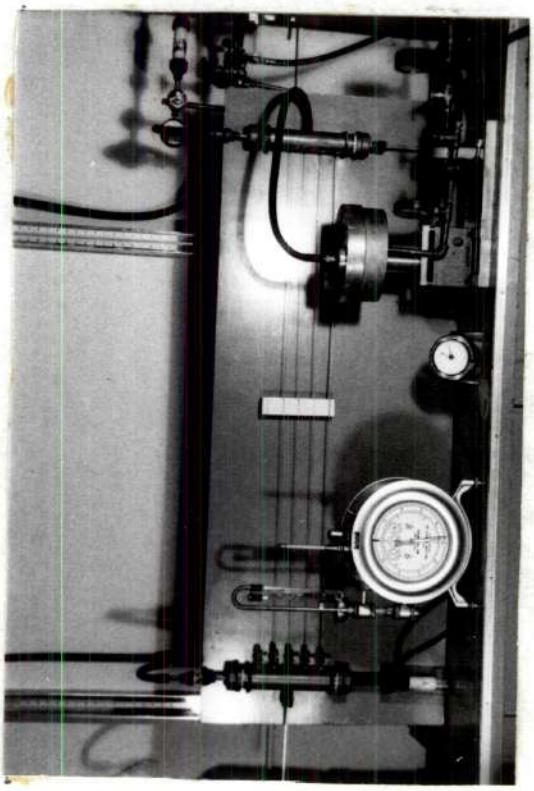

Fig. 2 Experimental Apparatus

diver was carefully tested and found to function in a very ineffective manner. This was the case, since the Cartesian diver, which attempts to reduce the pressure by a bleeding action, had a very limited bleeding capacity. Therefore, the familiar self-operated diaphram type pressure regulator is employed in the final apparatus design for supplying air at constant pressure.

Fig. 1 shows two such regulators operating in series to provide a very constant pressure air supply to the system, though the source pressure varies from 90 to 120 pounds per square inch gage. Such operation is justified since it divides the regulation between these two ratio type controllers. Pressure gages and globe valves are assembled as shown so that regulation can be divided and any required pressure may be supplied to the system. An air filter, packed with glass wool, is placed in the air line to remove any foreign matter which might tend to clog the capillary tubes. Also, it is noted that a large regulator, valves, and gage are so connected that any air pressure desired may be supplied to the air motor. The on-off valve allows the air motor to be turned on and off instantly, while the air motor's speed may be preset by adjusting the regulator, which supplies the motor with air.

The cloud generator is a device capable of creating an aerosol from fine powder and air which are supplied to the generator. It is seen in Fig. 1 to consist of at

least five essential parts. First, there is an air motor which may be operated at various speeds depending upon the pressure of the air supplied to it. Second, there is a set of gears, which ratio down the speed of the air motor about ten to one. Third, there is a circular felt disk which is motivated by the output of the gear train. By varying the pressure supplied to the air motor, this disk may be rotated at speeds from zero to two revolutions per minute. Fourth, there is an air tight cylinder which encloses the rotating felt disk. Air can be made to enter below the disk and allowed to exit above the disk. Fifth, there is a brush which is proximate to the upper surface of the disk.

In operation, the cap is removed and the generator charged with a quantity of very fine powder. The cap is then replaced, thus making the cylinder again air tight. The air motor is turned on and the felt disk is caused to rotate by means of the gear train. As the disk rotates, the stationary brush causes a thin layer of powder to cover the surface of the disk. Excess powder piles up behind the brush and the dam assembly, which is not shown. As air is supplied to the air inlet below the disk, it flows through the porous disk, picking up powder from the layer and then carrying the powder along as it exits through the outlet above the disk. By varying the R.P.M. of the disk and the flow rate of the air, suspensions of

different solids concentrations should be obtained. Fig. 3 is a photograph showing the exterior of this cloud generator.

The two manifolds shown in Fig. 1 are made from standard two inch copper pipe. These 18 inch long pipes are drilled and tapped to provide the necessary connections. Standard brass caps, drilled and tapped, form the tops and bottoms of these manifolds. Standard quarter-inch brass valves, with male pipe threads on both ends, are connected to Manifold No. 2. Quarter-inch brass caps are drilled to fit the capillary tubes and then tightened onto the five valves. Manifold No. 1 is drilled with the corresponding size holes. The capillary tubes are fitted in the proper holes and are carefully soldered into place. The nominal diameters of the seamless nickel tubing are given as follows: (Z, 0.010 in. I.D., 0.020 in. O.D.); (A, 0.020 in. I.D., 0.062 in. O.D.); (B, 0.040 in. I.D., 0.062 in. O.D.); (C, 0.052 in. I.D., 0.072 in. O.D.); and (D, 0.082 in. I.D., 0.096 in. O.D.). The nominal length of these five small diameter tubes is four feet. Tube No. Z is so numbered because it was found to be clogged from the very beginning and thus no data were obtained from it.

The approximate gas temperature in each manifold is measured by mercury thermometers of the laboratory type. A drilled pipe cap containing a one-hole rubber stopper

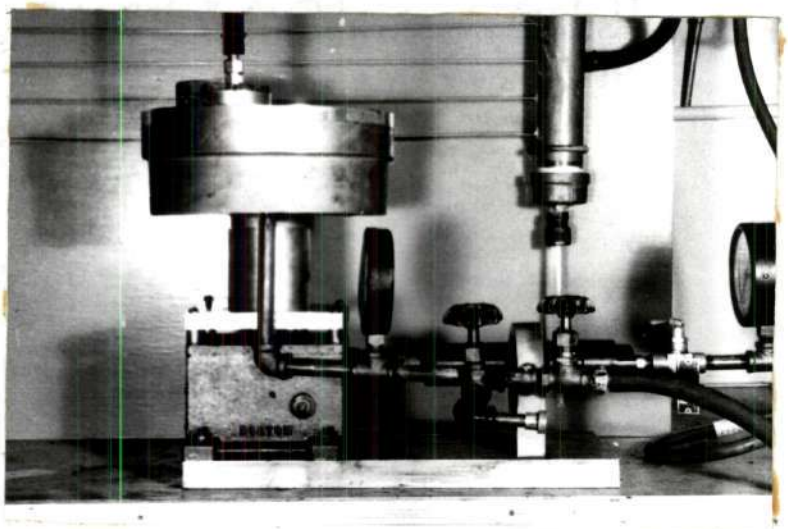

Fig. 3 Cloud Generator

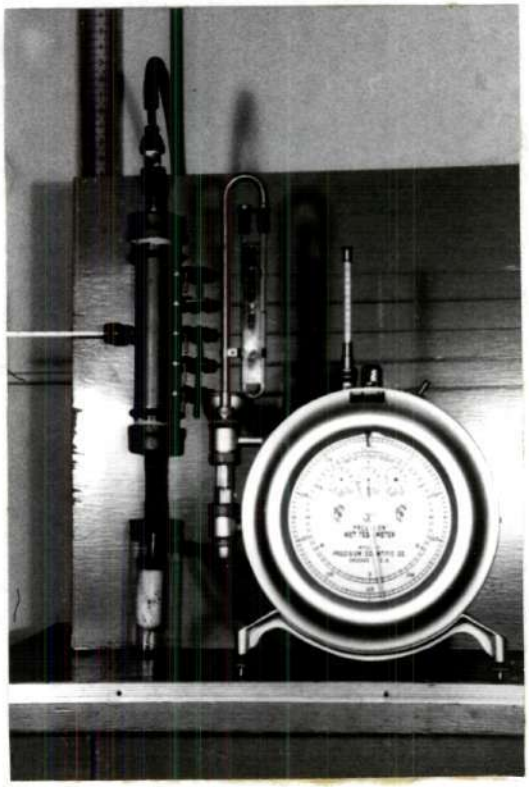

Fig. 4 Separation and
Metering Equipment

forms the gasket assembly for these long-stem glass thermometers. The pressure in the manifolds is measured by two commercial manometers. Manometer No. 1 is a mercury manometer which measures gage pressures up to thirty inches of mercury. Manometer No. 2 is a water manometer which reads up to thirty inches of water. In each line, from manifold to manometer, an air filter is placed to keep the powder away from the manometers.

Separation of the solids from the air takes place in a thimble filter. The air stream passes on through the filter and into the wet test meter where it is measured. The solids remain in the thimble filter where they are measured by difference weighings on an analytical balance. The filter container is made of glass so that any leakage of solids may be detected visually. The conditions of pressure and temperature in the wet test meter are measured by Manometer No. 3 and Thermometer No. 3 respectively. The time for collection is measured with a mechanical timer, which reads to the tenth of a second. This separating and metering section is shown photographically in Fig. 4.

Material. — The material used to form the aerosols in this thesis project is a very fine carbon powder with a specific gravity given as 2.26. A sample of an aerosol produced with the powder was collected with a thermal

precipitator on electron microscope grids and electron microphotographs were made. The results of a particle count made from these microphotographs are plotted on a probability grid which is shown in Fig. 14 in the Appendix. From this plot it is seen that 85 per cent of the particles are less than one micron in diameter and 60 per cent are less than a half-micron in diameter. In calculating, using the method given by DallaValle (6), the geometric mean diameter, G is the 50 per cent size and the geometric standard deviation, σ_g, is found by the equation:

$$\sigma_g = \frac{84.13 \text{ per cent size}}{50 \text{ per cent size}} \qquad (19)$$

Since, the mean diameter, G, is by count, a mean diameter on the weight basis, d_w, must be calculated. This is done by using the equation given by DallaValle (6):

$$\ln d_w^4 = \ln G^4 + 8.0 \ln^2 \sigma_g \qquad (20)$$

However, there are still many more problems involving the particle size, as is discussed in Chapter IV. It is well to point out that this material tends to agglomerate and to bread up when flowing through the tubes. Thus, the particle diameter is an evasive quantity. Due to this agglomeration, the shapes of these particles are not

readily determinable.

No material other than the carbon powder described is employed in this experimental work, because it is felt advisable not to contaminate the borrowed cloud chamber with materials other than the carbon powder for which it is intended. This is further discussed in Chapter VI.

Experimental procedure. — The nominal diameter of the capillary tubing can not be taken as the true tube diameter, since any dents, bends, or other damage incurred in the shipping of the tubes or in the fabrication of the equipment would easily reduce the effective diameter of such fine diameter tubes. Thus, a series of preliminary runs is made using only air flow through the tubes. Runs are made using several air rates for each tube, with the exception of Tube No. Z, and all data taken including barometric pressure, manifold pressures and temperatures, wet test meter readings, temperature and pressure in the wet test meter, and time for the run. These data are included in the Appendix in Table 1. The effective tube diameter is calculated from these data as is shown in Sample Calculations.

The suspension data are obtained in the following manner. The cloud chamber is charged with the carbon powder. Then, with the on-off valve open, the air motor regulator is adjusted to give the desired disk R.P.M. and

then the on-off valve is closed. A thimble filter is carefully weighed with the analytical balance. With an extra thimble filter in place, the air supply to the cloud chamber is adjusted to give the desired manifold pressure as read on Manometer No. 1. The glass container is removed from the filter and the wet test meter set at zero. The weighed filter is now put in place and simultaneously, the glass container is put in place, the on-off valve of the cloud generator opened and the timer started. During the run, all pressures and temperatures are recorded. To conclude a run, simultaneously the timer is stopped, the on-off valve closed, the glass container removed, and the weighed filter replaced by the extra thimble filter. These simultaneous actions require that two operators perform them. The thimble filter is reweighed to find its gain in weight and the readings of the wet test meter and the timer are recorded. This procedure is followed to obtain many runs, using each tube at various air rates and solids concentrations. This is done by varying the pressure in Manifold No. 1 and varying the R.P.M. of the cloud generator. The data are listed in the Appendix in Table 3 and the calculations shown in the Appendix in Sample Calculations. The many difficulties inherent in this apparatus and this system are discussed in Chapter IV.

CHAPTER IV

DISCUSSION OF RESULTS

Gasterstadt correlation. — Values of α and R are calculated as shown in Sample Calculations and are tabulated in the Appendix in Table 4 and Table 5. These points are plotted on linear co-ordinates and shown in Fig. 5. No one straight line can be drawn through these points, since these points represent many different air velocities. Since data are so varied as far as air rate, no attempt is made to connect points of similar air rate.

In an effort to find if the Gasterstadt (9) straight line relation will correlate these points, another attack is tried. For each point in Fig. 5, the slope of a line from the origin ($R = 0, \alpha = 1$) through the point and the air rate, G_a, for each run are tabulated in Table 6 and Table 5. Fig. 6 shows a plot of these slopes versus the mass air rates.

There is evidence of a relation in Fig. 6 if certain points are left out. The points where R is very low (i.e. $R \leq 0.006$) are shown circled in Fig. 6. Thus, it appears that the plot of a single air rate, G_a, in Fig. 5 would curve into the origin ($R = 0, \alpha = 1$) rather than appear

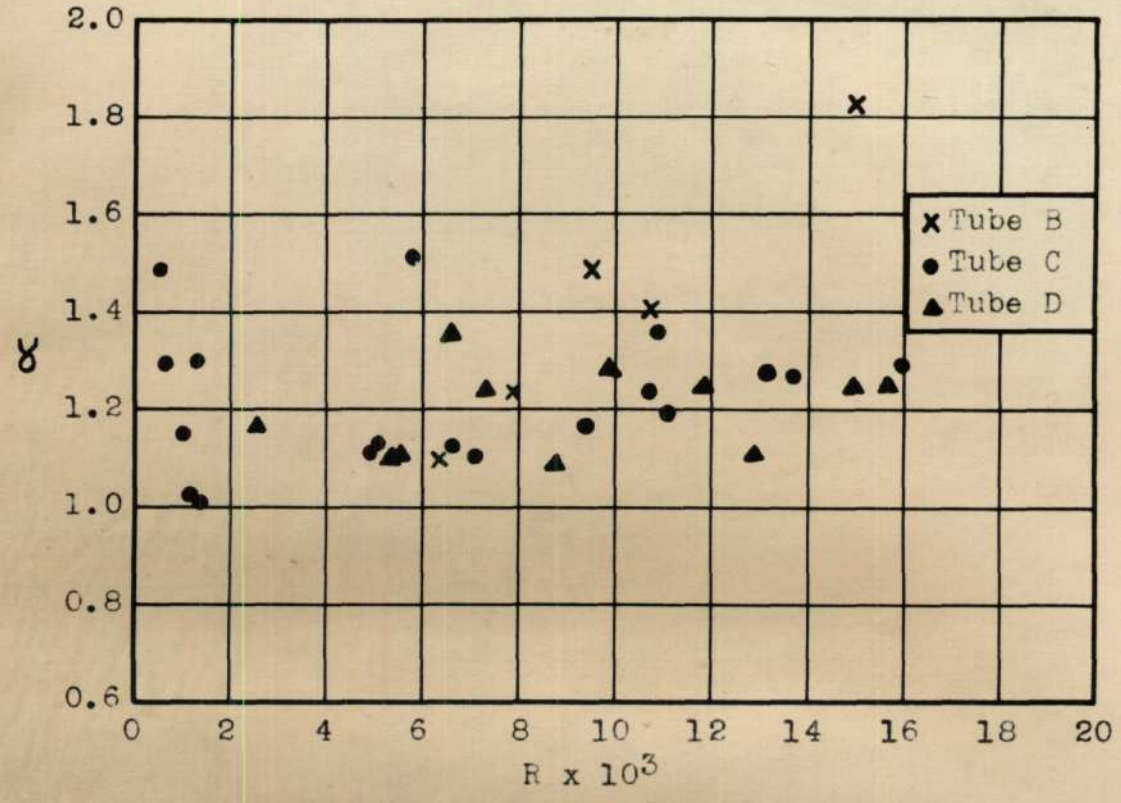

Fig. 5 Plot of Pressure Drop Ratio Versus Specific Loading

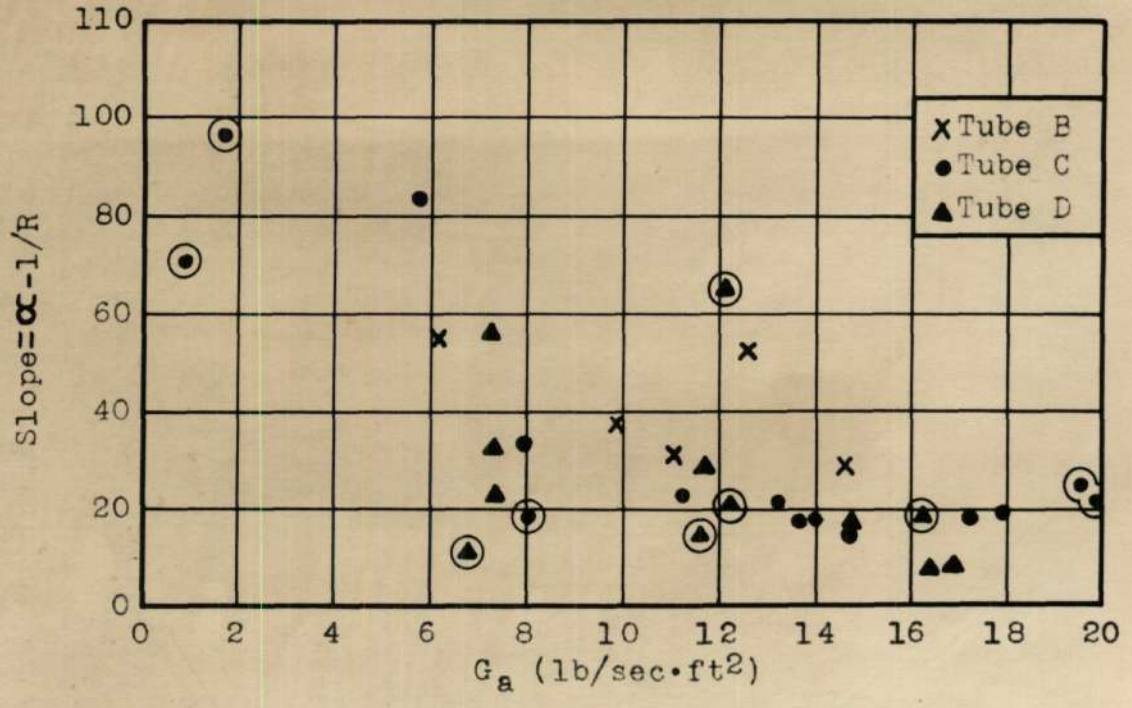

Fig. 6 Plot of Slope Versus Mass Rate of Air

as a straight line. This is the case because, for such a curved line, the slope of a line from the origin to a point where R is low would give values high or low depending on the shape of the curve. Therefore, it appears that Gasterstadt's correlation does not relate the data of this thesis.

Farbar correlation. — As shown above, the data of this thesis seem to bear out what Farbar (8) found. However, this thesis is considerably handicapped by not containing a number of runs of constant mass air velocity, so that the α versus R relation might be seen directly. No attempt is made to plot the total pressure drop versus the air rate, since the data of this thesis are for many values of R. Indirect correlation is very difficult, because the data of this thesis are for several tubes and include streamline, intermediate, and turbulent flow so that such a plot would not give continuous straight lines.

Vogt and White correlation. — In the manner of Vogt and White (19), values of α-1/R and $(Re)_a \rho_p / D_t^2 \rho_a$ are calculated and tabulated in Table 6 in the Appendix. These values are plotted on a log-log grid in Fig. 7. Other than in the streamline region, no trend can be detected in these points. This may be explained in two possible ways. First, Vogt and White's (19) data is only in the turbulent

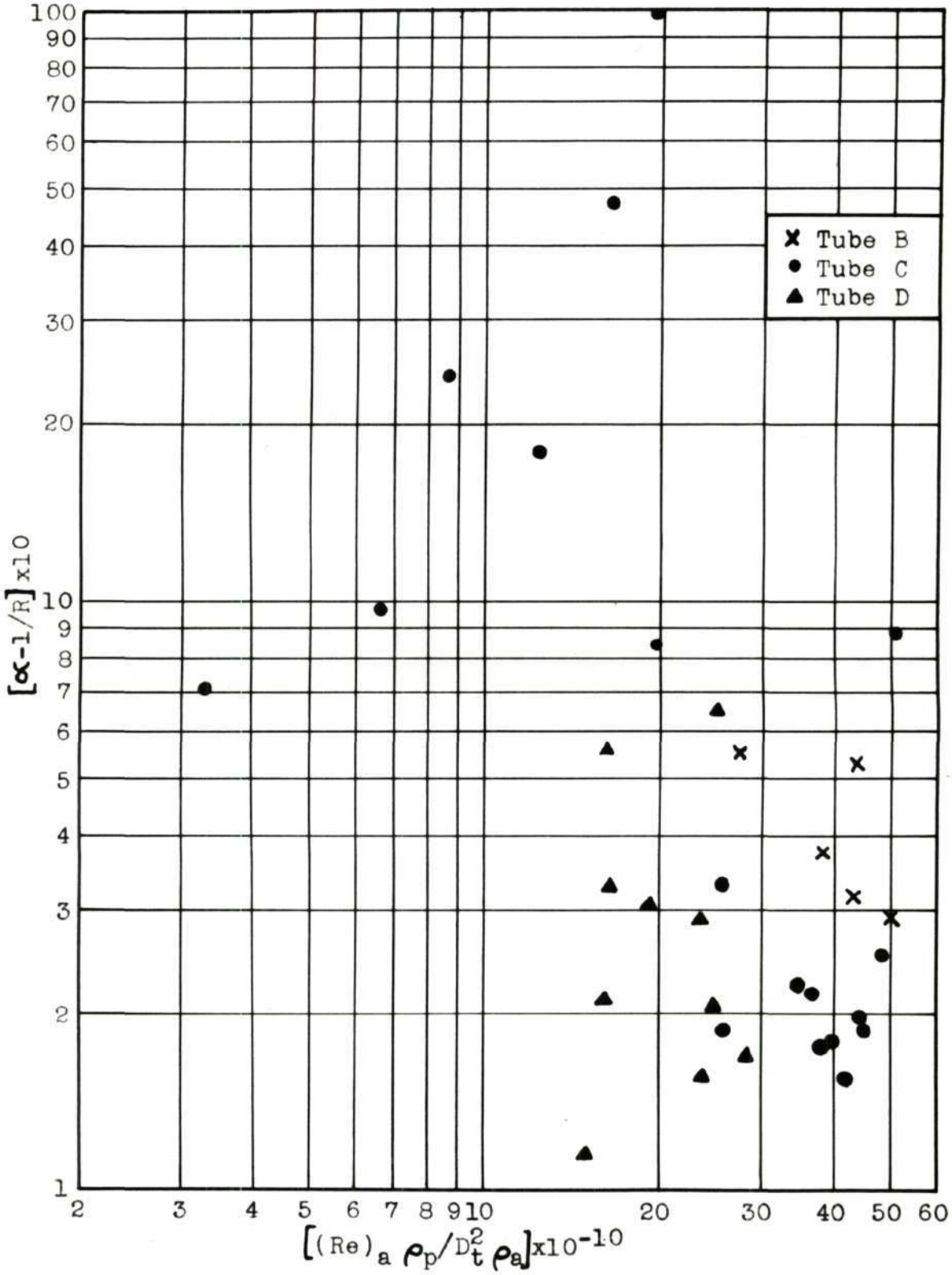

Fig. 7 Plot of Vogt and White Correlation

region, while this thesis covers the streamline and transition ranges also. Second, in computing the values plotted in Fig. 7, it is assumed that the particle diameter remains constant throughout all runs. This is probably not the case, as is discussed later in this chapter. The criticism of Belden and Kassel (2) about the Vogt and White (19) relation does not explain Fig. 7 since the data of this thesis were presumably obtained with some constant particle diameter. The points in the streamline region seem to curve upward. This seems to indicate that on such a plot as this, there will be a big discontinuity between the streamline and the turbulent sections. One reason for the points in the streamline section forming a fair line, while those in the other regions do not, is that these laminar points were very carefully obtained by making the runs extra long. See Table 3.

Belden and Kassel correlation. — Values of $f_A(Re)_a^{0.2}$ and $G_aG_p/(G_a+G_p)^2$ are calculated and listed in Table 6 of the Appendix. This is the correlation proposed by Belden and Kassel (2). In the Sample Calculations it is shown that the friction factor of Belden and Kassel is essentially the same as that of Lapple and Alves (14), f_A. In accordance with Belden and Kassel, the plot is made on linear co-ordinates and is shown in Fig. 8. There is a straight line of positive slope indicated by the points in the

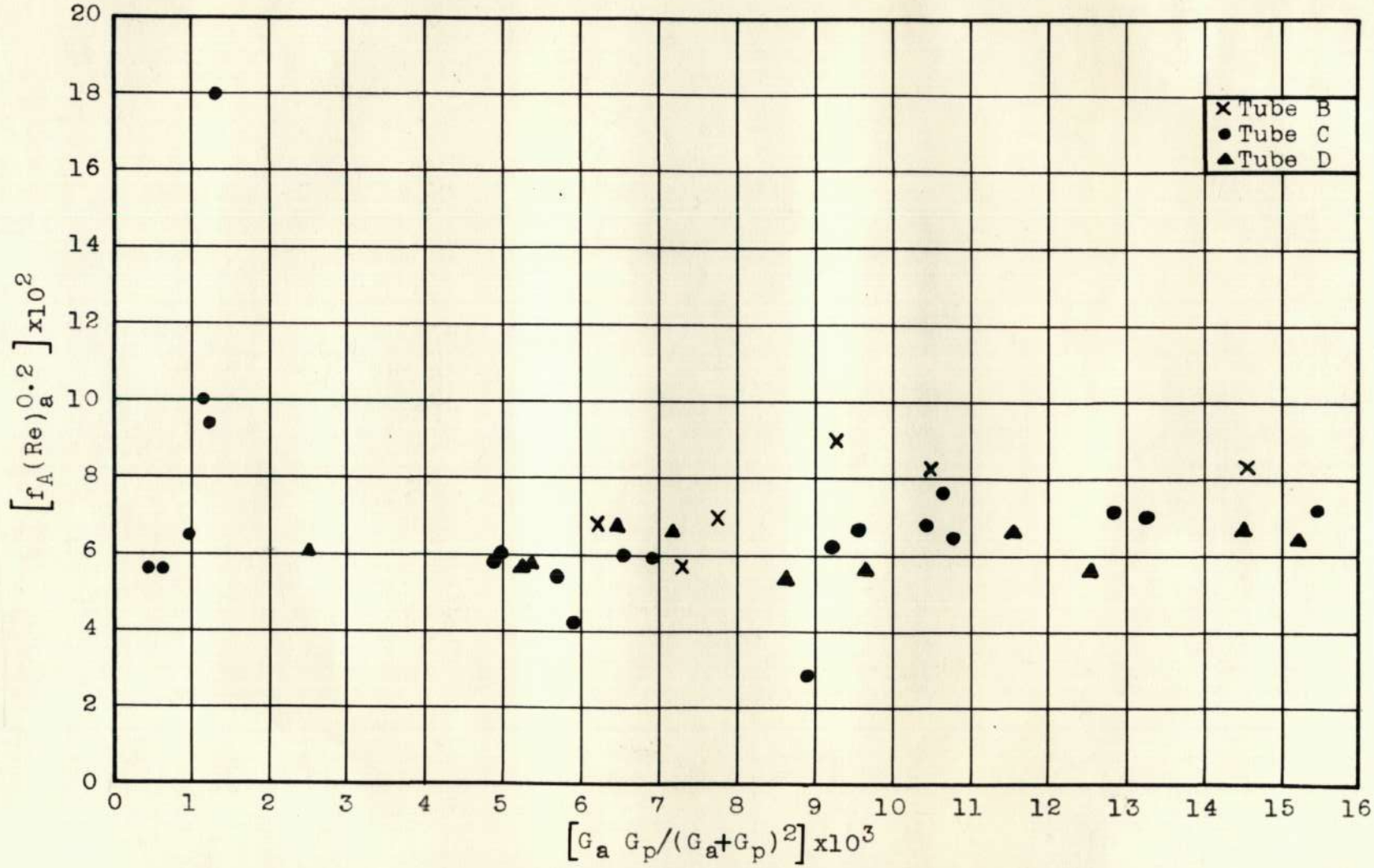

Fig. 8 Plot of Belden and Kassel Correlation

turbulent region. Though these points are in a lower range than those of Belden and Kassel, there is good agreement between these values and the extrapolated portion of the Belden and Kassel (2) plot. Here again, the streamline points tend to fall on a line of much higher slope. The indications are that there is a discontinuous section after the streamline points. However, if more points in the intermediate region had been obtained, a connection between the streamline and turbulent regions might have appeared. Also, values are calculated in the manner shown by the above workers for α-1 and $(Re)_a G_a/G_p$, which are tabulated in Table 4 and Table 6 in the Appendix. These values are shown plotted on a log-log grid in Fig. 9. Again the data of this thesis cover a wider range of Reynolds numbers but a narrower range of values of α-1, than those of Belden and Kassel. The plot is similar to that of Belden and Kassel (2) in that it tends to show a negative slope. The points are so scattered that little more can be said about this correlation.

Albright et al correlation. — The correlation of Albright et al (1) is checked by calculating values of α-1 and values of $(Re)_a \rho_p / R \rho_a D_t$, which are listed in Table 4 and Table 6 in the Appendix. These values are shown on a log-log grid in Fig. 10. Although the points are scattered, in general they give a line of negative slope. The plot of Albright

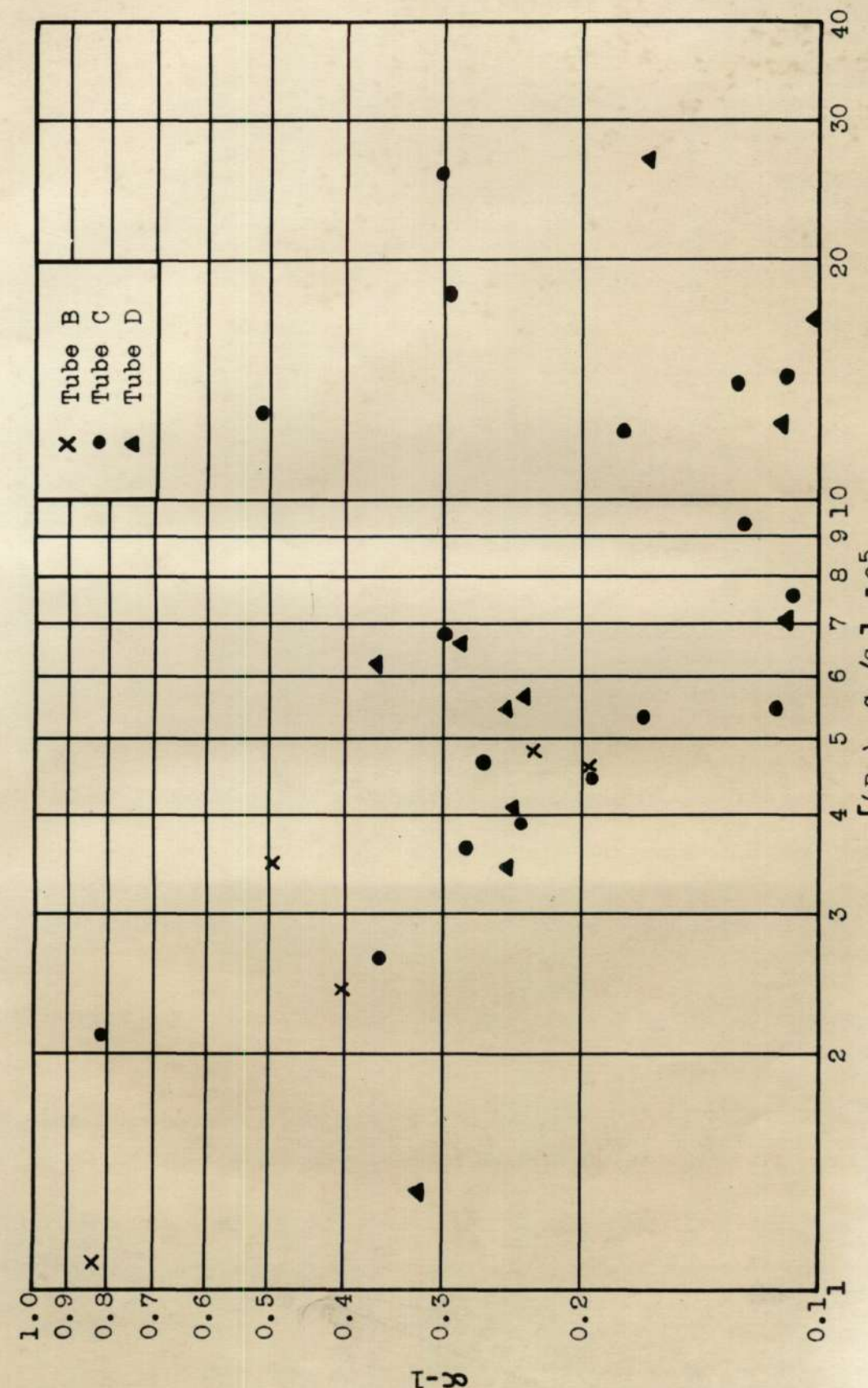

Fig. 9 Plot of Belden and Kassel Correlation

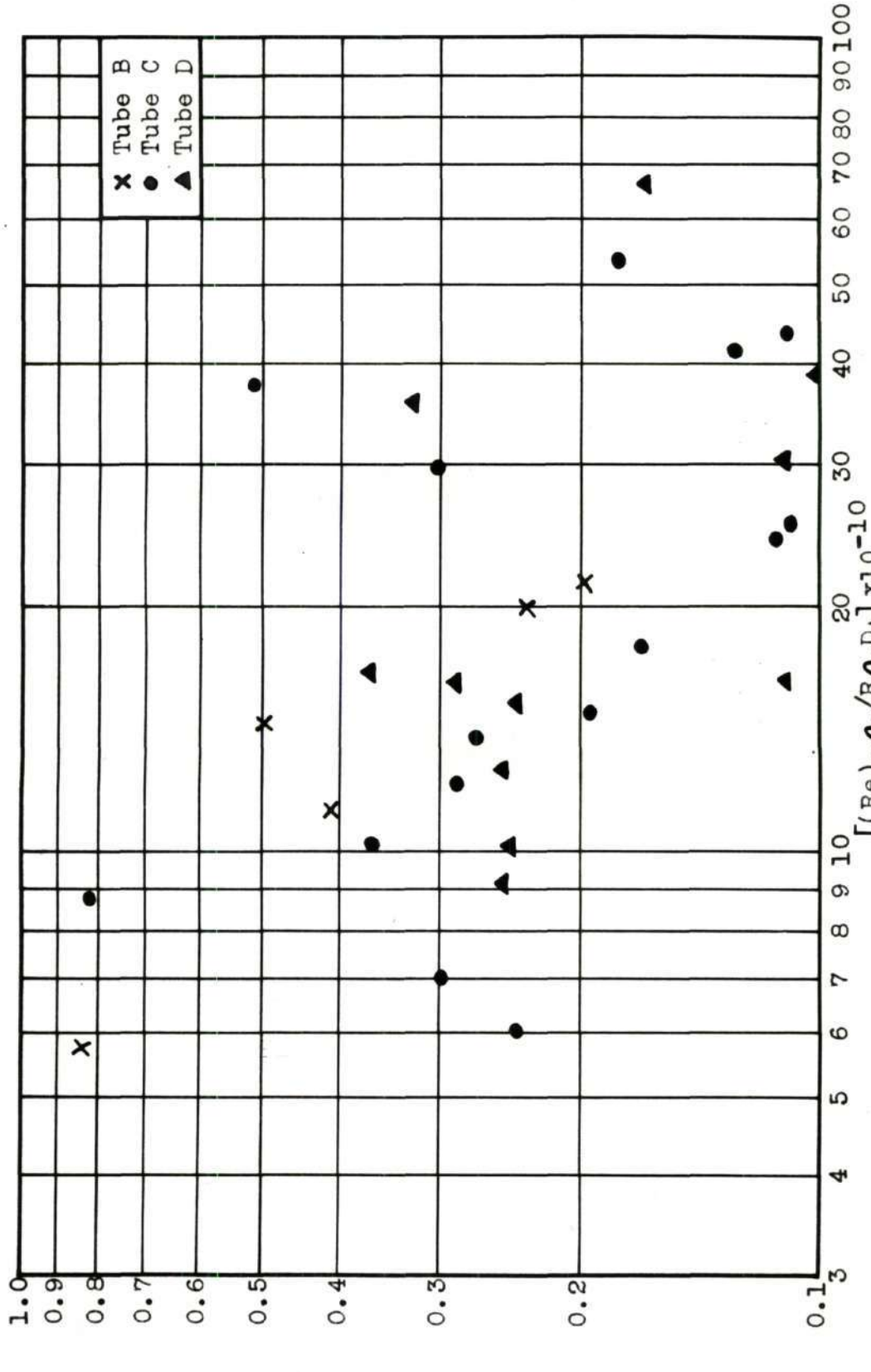

Fig. 10 Plot of Albright Correlation

et al (1) gives a curved line representing their data. These authors also propose a plot of friction factor versus G_{mean}. Both the factors of Lapple, Alves, et al (14) and of Culgan (5) are used in making the log-log plot shown in Fig. 11. The numerical values are tabulated in Table 5 and Table 6 of the Appendix. Though the points are scattered in the turbulent region, all three regions are represented. Just as in the plot given by Albright et al (1), separate lines are seen for the three different tube diameters.

Alves correlation. — Following the method proposed by Lapple, Alves, et al (14), values are calculated for f_A and $(Re)_m$ as defined in the Literature Review. These are tabulated in Table 5 in the Appendix and are plotted on log-log co-ordinates in Fig. 12. This is an excellent correlation showing all regions. However, the values of f_A are much higher than the corresponding values of Fanning friction factors, f_a. Thus, using f_a in design calculations would give values of pressure drop lower than the observed pressure drop. To illustrate this, a plot of calculated ΔP, using the Fanning friction factor, is made versus the observed ΔP on linear co-ordinates in Fig. 13. There are differences between the two of up to 40 per cent.

Culgan correlation. — Though Culgan (5) correlates his data in a somewhat empirical fashion, it is felt that his

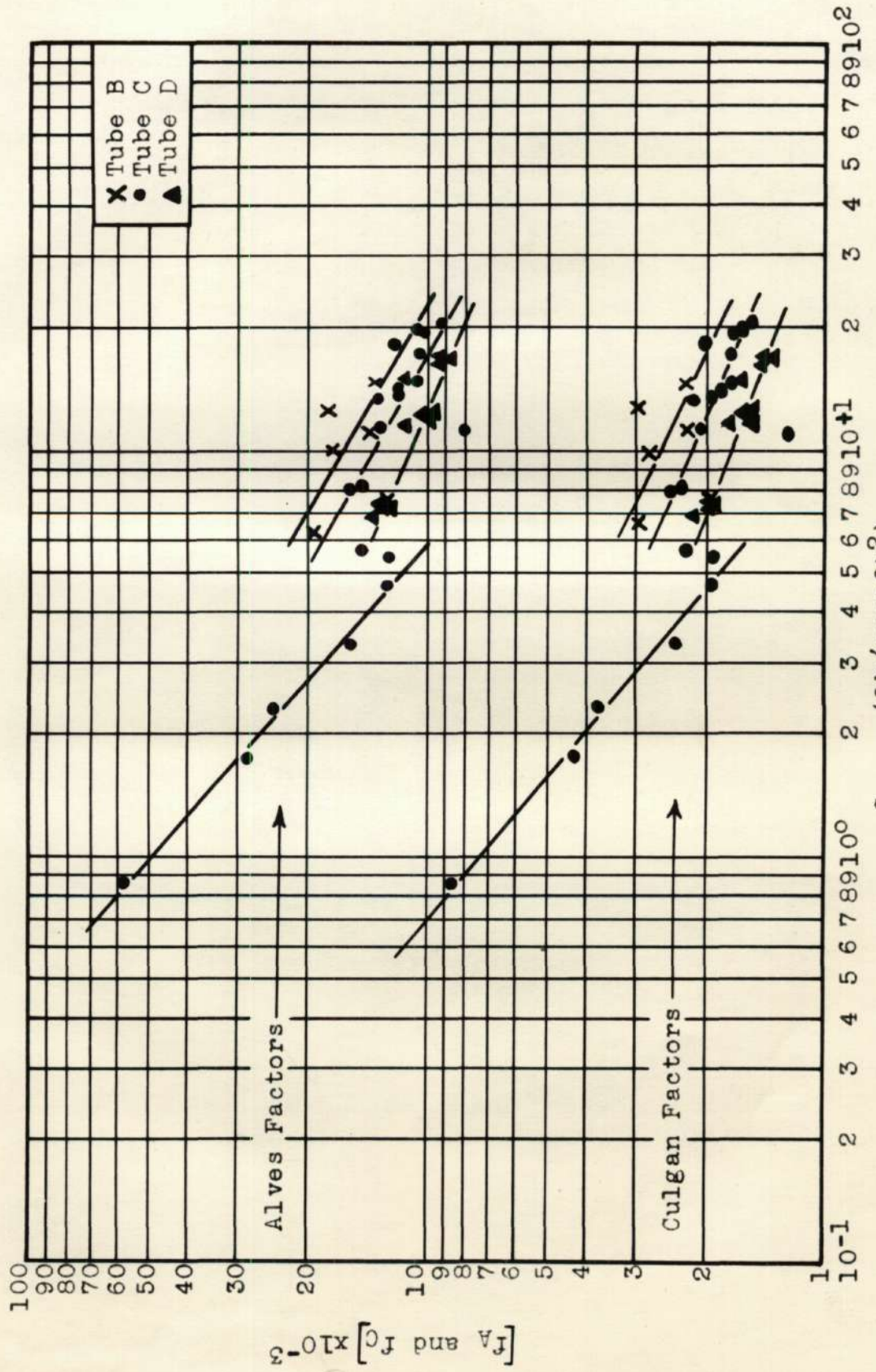

Fig. 11 Plot of Albright Correlation

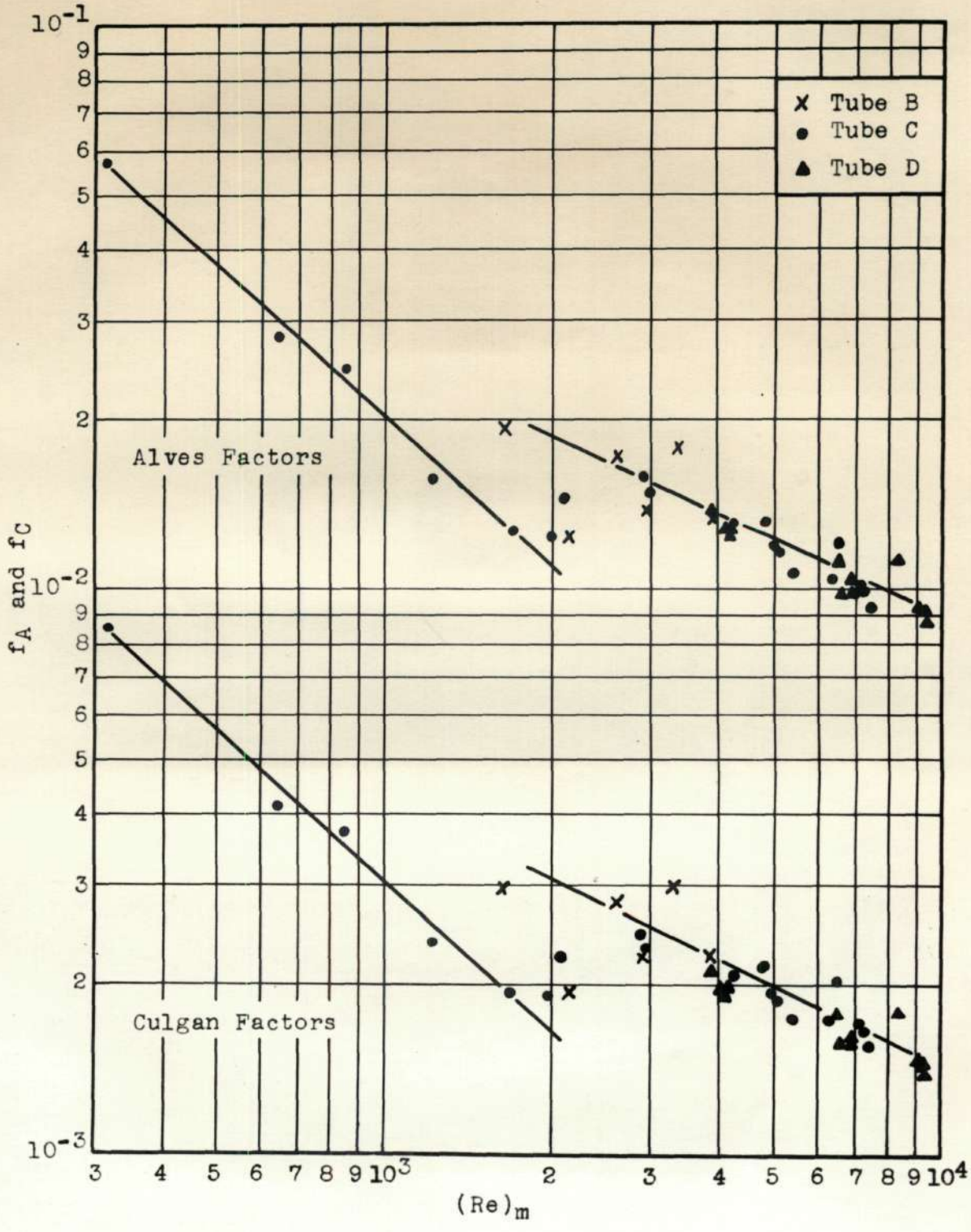

Fig. 12 Plot of Alves and Culgan Correlation

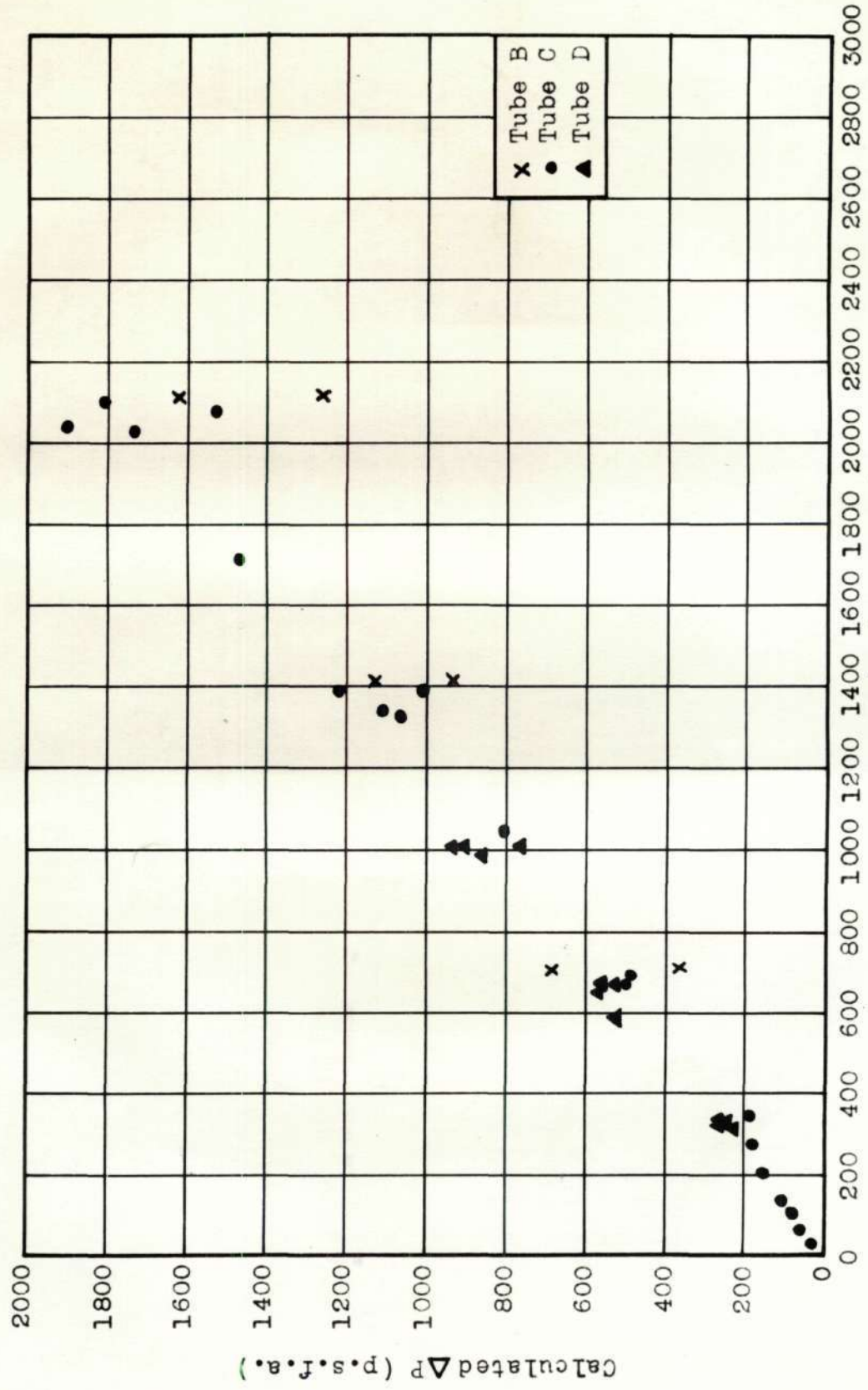

Fig. 13 Observed and Calculated Pressure Drops Compared

equation should also be tested. This equation is given in the Literature Review. Values of f_C and $(Re)_m$ are computed and then tabulated in Table 6 and Table 5. These values are plotted on the same grid as the Alves values in Fig. 12. The question occurs as to just what power should be used for particles with the density of carbon. Culgan's friction factor seems to offer no advantage over the Alves factor.

Hinkle correlation. — As was pointed out in the Literature Review, the plot proposed by Hinkle (11) has no meaning until the nature of the solids friction factor f_p, is investigated. If the method of Hinkle were used here, a straight line of unit slope is guaranteed.

Slip velocity. — One would suspect that particles one micron or less in diameter would travel at velocities very nearly the average velocity of the air stream. Since the particle velocities are not measured in this experimental work, such information would have to be calculated using principles set forth by other workers. If the particles are assumed to be all one diameter, an attempt might be made to calculate the slip velocities in each run, using the method outlined by Hinkle (11). This trial and error method utilizes the plots of C_D versus Reynolds number given by Perry (15) or DallaValle (6). Use of such a method gives very unreasonable answers for the data of

this thesis. This is so primarily because such plots give the drag coefficient for the single particle, $(C_D)_{single}$, while the drag coefficient for the cloud, $(C_D)_{cloud}$, is required. At the time of this writing, no relation between these two factors is available for the range of conditions encountered in this horizontal flow case. Equations such as:

$$u_p = u_a - u_{ff} \tag{19}$$

given by Chatley (3) and Lapple, Alves, et al (14), while only approximations, give a general idea of the magnitude of the slip velocity. The free fall velocity in air for a carbon sphere, one micron in diameter, is:

$$u_{ff} \cong 7 \times 10^{-3} \text{ ft/sec} \tag{20}$$

When this is compared with the air velocities which range from 12 to 185 feet per second, it is apparent that slip is probably negligible. In other words, this aerosol should behave somewhat like a true fluid.

Difficulties in the experimental system. — This section is not an attempt to run down the experimental system of this thesis, but to try to point out faults which should be remedied. Some of the remedies are discussed in the

chapter on Recommendations.

The pressure in Manifold No. 1 varies during a given run, though every attempt is made to keep it constant. This is true, since variations in the flow resistance of the cloud chamber cause variations in the manifold pressure even though the pressure supplied to the cloud generator is absolutely constant. This is caused by differences in thickness of the powder layer and other factors in the cloud chamber. It is not certain that the generator produces clouds with constant solids concentrations, even though the air pressures supplied to it are constant. Also, there is no assurance that the generator is not selective in the pickup of solids as far as size.

Although only an approximate temperature is required in each manifold, the placing of a lab thermometer in each manifold is certainly not the best method of measuring the temperature of the suspension.

From the very beginning of the experimental work, Tube No. Z was clogged. During the work, Tube No. B became clogged and neither of these tubes could be cleared. There is very good evidence that the carbon powder tends to break up when it is carried through a capillary tube in an air suspension. This is due to attrition between the particles. Such a phenomenon makes particle size a very elusive quantity.

The system of starting and stopping runs is not too

efficient and it requires two operators. Also, trouble is encountered when the thimble filter takes up moisture. This effect obscures the measurement of solids collected, if the amount of solids collected is small. Finally, large particles might have a tendency to settle and remain in the final manifold.

CHAPTER V

CONCLUSIONS

The following conclusions are drawn from material presented in this thesis:

1. Until such time as experimental information is presented on particle velocity and the nature of particle friction clarified, for the case of aerosol flow through capillary tubing, data are best correlated by the use of the Alves equation.

$$\Delta P_{ft} = \left(\frac{4 f_A \Delta L}{D_t}\right)\left(\frac{G_a^2}{2 g_c}\right)(1+R)\left(\frac{1}{\rho_a} + \frac{R}{\rho_p}\right) \qquad (6)$$

When f_A is plotted versus $(Re)_m$, the familiar Fanning type lines for the streamline, intermediate, and turbulent regions appear.

2. The Alves correlation is not recommended for design purposes, since equating the Fanning friction factor and the Alves friction factor will give calculated pressure drops as much as forty per cent lower than the observed pressure drops. Whether f_A will vary using different diameter particles, will be known only from further experimental work.

3. Since the Alves equation, which involves a modification of the Fanning equation, correlates the data of this thesis well, it appears that the aerosol behaves very much like a true fluid. With data on drag coefficients for clouds lacking, no calculation of slip velosity may be made. However, in the light of this aerosol's fluid-like behavior and such approximations as equation (19), it is concluded that the slip velocity, u_r, for the aerosol case is very small or negligible.

4. Theoretical equations, which involve slip velocity as a factor, will be of little value in correlating data for aerosol flow, since these equations become meaningless when u_r becomes zero. However, equations involving a friction factor for the mixture, such as those of Belden and Kassel (2), Albright et al (1), Lapple, Alves, et al (14), and Culgan (5), will become valuable for aerosol flow calculations when sufficient experimental data are presented to give certain values for such friction factors. The particle friction factor of Hinkle (11), with more investigation, will be more useful where the particle velocity may be more easily determined.

CHAPTER VI

RECOMMENDATIONS

This is a first attempt at obtaining pressure drop data for aerosol flow in capillary tubing, and thus many of the problems are brought to light. More data should be obtained from an improved experimental system. The new experimental data should cover a wide range of variables, so that a much better understanding of the effect of the variables on the pressure drop might be gained.

In an effort to surmount some of the difficulties mentioned in Chapter IV, the following improvements are suggested:

1. The pressure in Manifold No. 1 may be maintained at a more constant pressure and the solids concentration held more constant by operating the cloud generator at a fixed pressure drop. This might be done by supplying regulated air to Manifold No. 1 at some pressure less than the pressure supplied to the cloud chamber.

2. More accurate temperature measurements might be made and the system might be made essentially adiabatic.

3. By including an air dryer and by removing any possible large particles from the powder, clogging of the

capillary tubing might be prevented.

4. A different aerosol not so subject to agglomeration and breakup should be selected. Also, this material should be within narrow limits, particles of the same diameter. Materials of different densities should be tested.

5. A more efficient system of collecting and weighing the solids should be devised.

6. Data covering a wide range of values of particle diameter, tube size, air rate, solids concentration, and particle density should be obtained. At least four of these variables should be held constant while the other is varied and the pressure drop measured.

7. A longer length of tubing with several pressure taps should be employed, so that pressure measurements across a constant velocity section can be assured.

8. If possible, an attempt to measure particle velocity should be made. The problems involved in this are not discussed.

9. Finally, as more accurate experimental data are obtained, they should be either correlated with previously presented equations or an equation should be proposed which represents the data.

SAMPLE CALCULATIONS*

A. AIR RUN CALCULATIONS (Run No. 20 is illustrated.)

1. Dry Air Rate —
From temperature in test meter, T_3, the vapor pressure of water at this temperature is found from Perry (15), p. 149. Since pressures are low, perfect gases and Dalton's Law are assumed. Also, correction to average conditions in the capillary is made.

$$Q_a = \frac{(\text{Meter Vol.})(P_3 - P_s)(T_{mean})}{(T_3)(t)(P_{mean})} = 0.00566 \text{ ft}^3/\text{sec} \quad (21)$$

2. Average Gas Density —
Perfect gas is assumed since pressures are low:

$$\rho_a = \frac{(P_{mean})(M)}{(R_o)(T_{mean})} = 0.0839 \text{ lb-mass/ft}^3 \quad (22)$$

3. Friction Factor —
If point is in the streamline region equation is:

$$f_a = \frac{16}{(Re)_a} \quad (23)$$

Since Run No. 20 is in the turbulent region,

---

*All units are English Units as shown in the Symbols Section. Conversion of units from one system to another is not shown in Sample Calculations.

Koo's equation in Perry (15) p. 383 is used:

$$f_a = 0.0014 + 0.125(Re)_a^{-0.32} = 0.0014 + 0.5716\, D_t^{0.32} \quad (24)$$

Viscosity is taken from p. 371 of Perry (15).

4. Weymouth Equation —
This equation is used since a perfect gas is flowing at essentially constant temperature. See Perry (15) p. 383.

$$P_1^2 - P_2^2 = \frac{4 f_a L Q_a^2 \rho_a R_o T_{mean}}{D_t g_c M A_t^2} \quad (25)$$

Solving for Run No. 20:

$$f_a = 6.39 \times 10^8\, D_t^5 \quad (26)$$

5. Solution for D_t —
Trial and error solution of equation (24) and (26) give values.

$$D_t = 6.70 \times 10^{-3} \text{ft} = 0.0803 \text{ in} \quad (27)$$

B. SUSPENSION RUN CALCULATIONS (Run No. 69 is illustrated.)

1. Fundamental Values —

Air Rate is calculated as in Air Run Calculations:

$$Q_a = \frac{(\text{Meter Vol.})(P_3 - P_s)(T_{mean})}{(T_3)(t)(P_{mean})} = 0.001048 \text{ ft}^3/\text{sec} \quad (28)$$

Mean Density:

$$\rho_a = \frac{(P_{mean})(M)}{(R_o)(T_{mean})} \simeq 0.0772 \text{ lb-mass/ft}^3 \qquad (29)$$

Air Mass Rate:

$$G_a = Q_a \rho_a / A_t = 5.48 \text{ lb-mass/ft}^2\text{sec} \qquad (30)$$

Solids Mass Rate:

$$G_p = \frac{(\text{Solids Wt.})}{(A_t)(t)} = 2.69 \times 10^{-3} \text{lb-mass/ft}^2\text{sec} \qquad (31)$$

Air Velocity:

$$u_a = Q_a / A_t = 71.0 \text{ ft/sec} \qquad (32)$$

Air Friction Factor:
Just as illustrated in the Air Run Calculations, for runs in the turbulent region, Koo's equation is used. For streamline case have:

$$f_a = 16/(Re)_a = 8.10 \times 10^{-3} \qquad (33)$$

Pressure Drop due to Air Friction:
The Weymouth equation is used.

$$P_x^2 = P_2^2 + \frac{4 f_a L Q_a^2 \rho_a^2 R_o T_{mean}}{D_t g_c M A_t^2} = 2257 \text{ psfa} \qquad (34)$$

Then:

$$\Delta P_{fa} = P_x - P_2 = 189 \text{ psfa} \qquad (35)$$

2. Gasterstadt Values —

Pressure Drop Ratio:

$$\alpha = \Delta P_{ft}/\Delta P_{fa} = 1.483 \tag{36}$$

Specific Loading:

$$R = W_p/W_a = G_p/G_a = 4.90 \times 10^{-4} \tag{37}$$

Slope of Lines on Gasterstadt Plot (Fig. 6):

$$\text{Slope} = \alpha - 1/R = 19.71 \tag{38}$$

3. Vogt and White Values —

$$\alpha - 1/R = 19.71 \tag{39}$$

$$(Re)_a \rho_p/\rho_a D_t^2 = 1.924 \times 10^{11} \text{ ft}^{-2} \tag{40}$$

4. Belden and Kassel Values —

Since $G_p = R G_a$ and $G_a = u_a \rho_a$ have:

$$\frac{dP_{ft}}{dL} \quad \frac{2f(G_a + G_p)u_a}{g_c D_t} \quad \frac{2f G_a^2 (1+R)}{g_c D_t \rho_a} \tag{41}$$

Or:

$$f = \frac{\Delta P_{ft} g_c D_t \rho_a}{2 \Delta L G_a^2 (1+R)} \tag{42}$$

Where R/ρ_p term is negligible:

$$f_A \equiv \frac{\Delta P_{ft}\, g_c\, D_t}{2\Delta L\, G_a^2 (1+R)} \cdot \frac{1}{(1/\rho_a + R/\rho_p)} \cong f \qquad (43)$$

$$f_A (Re)_a^{0.2} = 0.0568 \qquad (44)$$

$$\frac{G_a G_p}{(G_a+G_p)^2} = \frac{R}{(1+R)^2} = 0.000489 \qquad (45)$$

$$(Re)_a\, G_a/G_p = (Re)_a/R = 4.03 \times 10^6 \qquad (46)$$

5. Albright et al Values —

$$\frac{(Re)_a \rho_p}{R\, \rho_a\, D_t} = 1.70 \times 10^{12}\ ft^{-1} \qquad (47)$$

6. Alves Values —

$$f_A = \frac{\Delta P_{ft}\, g_c\, D_t}{2\Delta L\, G_a^2 (1+R)} \cdot \frac{1}{(1/\rho_a + R/\rho_p)} = 1.249 \times 10^{-2} \qquad (48)$$

$$(Re)_m = (Re)_a (1+R) = 1.973 \times 10^3 \qquad (49)$$

$$(\Delta P_{ft})_{calc.} = \left(\frac{4f\Delta L\, G_a^2}{2 g_c\, D_t}\right)(1+R)\left(\frac{1}{\rho_a} + \frac{R}{\rho_p}\right) = 181.2 psfa \qquad (50)$$

7. Culgan Values —

$$\rho_m = \rho_a + \rho_{ds} = \rho_a + \frac{W_p u_a}{W_a u_p}\rho_a = \rho_a\left(1 + R\frac{u_a}{u_p}\right) \qquad (51)$$

Hinkle (11) on p. 16 is correct in his criticism of Culgan's thesis. However, since in this thesis u_p is unknown and for these very small particles $u_p \rightarrow u_a$, it will be assumed that $u_p = u_a$. Thus, in the manner of Culgan, the mean density is calculated from:

$$\rho_m = \rho_a(1+R) = 0.0772 \text{ lb-mass/ft}^3 \qquad (52)$$

Culgan's Friction Factor:

$$f_C = \frac{2g_c D_t h_m}{u_a^2 \Delta L(1+R)}\left(\frac{\rho_m}{\rho_p}\right)^{0.25} \frac{2g_c D_t \rho_a \Delta P}{G_a^2 \Delta L(1+R)}\left(\frac{\rho_m}{\rho_p}\right)^{0.25} \qquad (53)$$

If R/ρ_p term in the Alves equation is negligible then:

$$f_A = \frac{\Delta P_{ft} g_c D_t}{2\Delta L G_a^2(1+R)} \cdot \frac{1}{(1/\rho_a + R/\rho_p)} \cong f_C\left(\frac{\rho_m}{\rho_p}\right)^{-0.25} \qquad (54)$$

$$f_C = f_A\left(\frac{\rho_m}{\rho_p}\right)^{0.25} = 1.909 \times 10^{-3} \qquad (55)$$

TABLE 1.

EXPERIMENTAL DATA FOR AIR RUNS

Barometric Pressure: 731 mm. Hg

Run & Tube Nos.	Gas Meter Start (ft^3)	Gas Meter Finish (ft^3)	Press. No.1 (in. Hg)	Press. No.2 (in. H_2O)	Press. No.3 (in. H_2O)	Temp. No.1 (^oC)	Temp. No.2 (^oC)	Temp. No.3 (^oF)	Time of Run (sec)
1 A	0.015	0.025	5.1	0.14	0.04	24.0	24.5	74.5	226.2
2 A	0.060	0.085	10.0	0.20	0.06	24.3	24.3	74.5	239.1
3 A	0.120	0.142	15.0	0.16	0.06	24.2	24.2	74.5	119.0
4 A	0.200	0.230	20.0	0.16	0.06	24.3	24.3	74.7	117.0
5 A	0.330	0.365	25.0	0.20	0.08	24.3	24.3	74.7	103.2
6 A	0.510	0.540	30.0	0.18	0.06	24.5	24.4	74.8	70.2
7 B	0.690	0.790	5.0	0.24	0.06	24.2	24.2	74.8	159.7
8 B	1.000	1.150	10.0	0.30	0.06	24.5	24.5	74.8	131.3
9 B	1.500	1.700	15.0	0.30	0.06	24.7	24.5	74.8	152.2
10 B	2.100	2.300	20.0	0.32	0.06	24.7	24.6	74.9	135.1
11 B	2.800	3.000	25.0	0.36	0.06	24.8	24.6	74.9	116.2
12 B	3.450	3.650	30.0	0.46	0.06	24.9	24.7	74.9	101.8
13 C	4.000	4.200	5.0	0.38	0.06	24.5	24.5	74.9	129.2
14 C	4.600	4.850	10.0	0.56	0.06	24.8	24.4	74.9	112.8
15 C	5.300	5.600	15.0	0.66	0.06	24.8	24.5	74.8	114.9
16 C	6.200	6.550	20.0	0.96	0.06	24.7	24.3	74.8	99.6
17 C	7.300	7.700	25.0	1.16	0.06	24.7	24.2	74.7	97.3
18 C	8.400	8.800	30.0	1.44	0.06	24.6	24.2	74.5	85.8
19 D	0.400	1.000	5.0	1.36	0.06	24.1	24.0	74.2	133.1
20 D	2.100	2.900	10.0	2.80	0.06	24.3	23.9	73.8	117.0
21 D	0.500	1.500	15.0	4.50	0.20	23.8	23.8	73.2	114.7
22 D	7.500	8.800	20.0	6.36	0.16	24.3	23.8	73.3	122.6

TABLE 2.

TUBE DIAMETERS CALCULATED FROM AIR RUN DATA

Run No.	Tube No.	Calculated Diameter(in)	Average Diameter	Per Cent* from Average	Nominal Diameter(in)
1	A	0.0193		-2.97	
2	A	0.0198		-0.45	
3	A	0.0203	0.0199"	+2.06	0.0200
4	A	0.0202	(0.001658')	+1.38	
5	A	0.0201		+1.06	
6	A	0.0197		-0.96	
7	B	0.0376		-1.00	
8	B	x.xxxx[a]		———	
9	B	x.xxxx[a]	0.0379"	———	0.0400
10	B	0.0384	(0.003165')	+1.11	
11	B	0.0382		+0.58	
12	B	0.0377		-0.74	
13	C	x.xxxx[a]		———	
14	C	0.0532		+2.03	
15	C	0.0509	0.0521"	-2.34	0.0520
16	C	0.0526	(0.004330')	+0.92	
17	C	0.0524		+0.54	
18	C	0.0515		-1.19	
19	D	0.0812		+0.53	
20	D	0.0803	0.0808"	-0.57	0.0820
21	D	0.0808	(0.006730')	+0.04	
22	D	x.xxxx[b]		———	

*The Koo equation only claims an accuracy of ±5 per cent.

[a]Run Numbers 8, 9, and 13 are omitted since they are in the transition region.

[b]Run Number 22 is omitted since the wet test meter capacity had been exceeded.

TABLE 3.

EXPERIMENTAL DATA FOR SUSPENSION RUNS

Run& Tube Nos.	Solids Weight (gm)	Gas Meter (ft^3)	Time of Run (sec)	Air Motor (RPM)	Press. No.1 (in. Hg)	Press. No.2 (in. H_2O)	Press. No.3 (in. H_2O)	Temp. No.1 (°C)	Temp. No.2 (°C)	Temp. No.3 (°F)	Bar. Press. (mm. Hg)
23 A	0.0033	0.0171	346.0	10	5.0	0.20	0.06	24.2	23.8	71.3	735.9
24 A	0.0013	0.0533	601.0	10	10.0	0.22	0.06	24.0	23.7	71.8	735.9
25 A	0.0100	0.0676	461.7	10	15.0	0.18	0.06	23.4	23.6	72.1	735.9
26 A	0.0034	0.0487	275.1	10	20.0	0.16	0.06	23.8	23.7	72.3	735.9
27 A	0.0035	0.0774	353.1	10	25.0	0.24	0.06	23.8	23.8	72.3	735.9
28 A	0.0070	0.0840	331.4	10	30.0	0.20	0.06	24.5	23.7	72.3	735.9
29 A	0.0073	0.0140	587.2	20	5.0	0.20	0.06	24.0	23.8	72.8	735.9
30 A	0.0007	0.0267	418.1	20	10.0	0.16	0.06	23.9	23.8	72.8	735.9
31 B	0.0485	0.2110	225.8	10	10.0	0.64	0.08	28.0	27.8	80.2	736.4
32 B	0.0462	0.2353	185.6	10	20.0	0.84	0.08	28.0	27.8	80.2	736.4
33 B	0.0809	0.3284	196.4	10	30.0	1.30	0.08	28.1	28.0	80.3	736.4
34 B	0.0648	0.1624	195.4	20	10.0	0.98	0.08	28.2	28.2	80.4	736.4
35 B	0.0695	0.2078	183.2	20	20.0	1.24	0.08	28.2	28.2	80.4	736.4
36 B	0.0801	0.2720	187.6	20	30.0	2.18	0.08	28.3	28.2	80.4	736.4
37 C	0.0720	0.2312	194.9	10	5.0	1.30	0.08	22.4	22.4	70.3	734.8
38 C	0.1067	0.3674	126.0	10	10.0	2.26	0.08	22.4	22.4	70.3	734.8
39 C	0.1604	0.4698	201.0	10	15.0	3.26	0.08	22.4	22.4	70.2	734.8
40 C	0.1059	0.4674	152.8	10	20.0	6.18	0.08	22.4	22.4	70.3	734.8
41 C	0.2470	1.1646	324.5	10	25.0	12.23	0.08	22.5	22.4	70.4	734.8
42 C	0.1150	0.7163	175.1	10	30.0	18.37	0.08	22.8	22.5	70.4	734.8
43 C	0.1109	0.3692	251.7	20	10.0	7.40	0.08	24.5	24.5	74.8	732.9
44 C	0.2996	0.8633	297.3	20	20.0	17.44	0.08	24.8	24.5	74.8	732.9
45 C	0.1549	0.8487	195.4	20	30.0	16.43	0.08	24.8	24.6	74.8	732.9
46 C	0.1635	0.3256	189.7	30	10.0	7.22	0.08	24.8	24.6	74.4	732.9

TABLE 3.

EXPERIMENTAL DATA FOR SUSPENSION RUNS

Run& Tube Nos.	Solids Weight (gm)	Gas Meter (ft^3)	Time of Run (sec)	Air Motor (RPM)	Press. No.1 (in. Hg)	Press. No.2 (in. H_2O)	Press. No.3 (in. H_2O)	Temp. No.1 (°C)	Temp. No.2 (°C)	Temp. No.3 (°F)	Bar. Press. (mm. Hg)
47 C	0.1640	0.5567	188.0	30	20.0	14.46	0.08	24.9	24.5	74.4	732.9
48 C	0.2290	1.4654	348.4	30	30.0	5.00	0.08	24.9	24.5	74.0	732.9
49 C	0.1079	0.3143	185.7	40	10.0	2.46	0.08	24.6	24.5	74.4	732.9
50 C	0.2231	0.5396	192.7	40	20.0	6.08	0.08	24.4	24.5	76.5	732.9
51 C	0.4614	1.0848	282.8	40	30.0	9.30	0.08	24.7	24.3	76.5	732.9
52 D	0.1043	0.9758	266.0	10	5.0	2.42	0.08	21.8	21.8	70.2	734.8
53 D	0.1295	1.5943	259.4	10	10.0	7.14	0.08	22.2	22.1	70.2	734.8
54 D	0.2597	1.5091	182.6	10	15.0	15.10	0.06	26.2	24.2	76.0	741.7
55 D	0.2688	0.7174	192.8	20	5.0	6.20	0.06	26.3	26.4	76.2	741.7
56 D	0.2523	0.8081	135.0	20	10.0	22.20	0.06	26.5	26.6	76.2	741.7
57 D	0.1354	0.4852	56.6	20	15.0	9.80	0.06	26.4	26.8	76.3	741.7
58 D	0.1459	0.6443	167.6	30	5.0	4.00	0.06	26.8	27.2	76.4	741.7
59 D	0.1256	0.7247	116.5	30	10.0	10.80	0.06	27.0	27.2	76.6	741.7
60 D	0.3289	0.8063	96.4	30	15.0	9.40	0.06	27.2	27.4	76.8	741.7
61 D	0.3695	0.4151	120.1	40	5.0	9.00	0.06	27.3	27.4	77.1	741.7
62 D	0.2720	0.5508	92.8	40	10.0	6.40	0.06	27.3	27.6	77.2	741.7
63 D	0.3270	0.6918	91.7	40	15.0	10.80	0.06	27.4	27.6	77.3	741.7
64 C	0.0071	0.1658	900.0	10	0.5	0.18	0.06	26.0	26.4	76.4	741.6
65 C	0.0124	0.3338	900.3	10	1.0	0.32	0.06	25.8	26.2	76.5	741.6
66 C	0.0175	0.4927	900.6	10	1.5	0.37	0.06	25.7	25.8	76.5	741.6
67 C	0.0135	0.4273	600.6	10	2.0	0.50	0.06	25.6	25.7	76.6	741.6
68 C	0.0124	0.5922	602.0	10	3.0	0.54	0.06	25.3	25.5	76.6	741.6
69 C	0.0108	0.6947	601.5	10	4.0	0.65	0.06	25.2	25.3	76.6	741.6

TABLE 4.

CALCULATED DATA FOR SUSPENSION RUNS

P_1 (psfa)	P_2 (psfa)	ΔP_{ft} (psf)	ΔP_{fa} (psf)	ΔP_{fp} (psf)	$(\Delta P_{ft})_{calc.}$ (psf)	α	$\alpha-1$	T_m (^oR)	ρ_a (lb/ft^3)	Run & Tube No.
2,759	2,055	704	XX	XX	688	XX	XX	542.0	0.0834	31 B
3,467	2,056	1,411	1,179	232	1,132	1.197	0.197	542.3	0.0957	32 B
4,174	2,059	2,115	1,719	396	1,621	1.231	0.231	542.5	0.1078	33 B
2,759	2,057	702	383	319	363	1.832	0.832	542.7	0.0833	34 B
3,467	2,058	1,409	1,002	407	937	1.407	0.407	542.7	0.0957	35 B
4,174	2,063	2,111	1,412	699	1,265	1.496	0.496	542.8	0.1078	36 B
2,399	2,052	347	191	156	185	1.818	0.818	532.3	0.0785	37 C
2,752	2,057	695	145	550	1,282	4.790	3.790	532.3	0.0848	38 C
3,106	2,062	1,044	843	201	807	1.239	0.239	532.3	0.0913	39 C
3,460	2,077	1,383	1,248	135	1,219	1.108	0.108	532.3	0.0977	40 C
3,813	2,109	1,704	1,516	188	1,468	1.125	0.125	532.4	0.1043	41 C
4,167	2,141	2,026	1,799	227	1,736	1.127	0.127	532.8	0.1110	42 C
2,747	2,079	666	XX	XX	852	XX	XX	536.2	0.0846	43 C
3,455	2,131	1,324	1,109	215	1,072	1.194	0.194	536.4	0.0977	44 C
4,162	2,125	2,037	1,349	688	1,901	1.511	0.511	536.5	0.1102	45 C
2,747	2,078	669	516	153	504	1.298	0.298	536.5	0.0844	46 C
3,455	2,115	1,340	1,148	192	1,111	1.167	0.167	536.5	0.0976	47 C
4,162	2,066	2,096	1,889	207	1,812	1.110	0.110	536.5	0.1090	48 C
2,747	2,053	694	510	184	493	1.362	0.362	536.2	0.0841	49 C
3,455	2,072	1,383	1,080	303	1,017	1.282	0.282	536.0	0.0976	50 C
4,162	2,088	2,074	1,633	441	1,530	1.269	0.269	536.1	0.1096	51 C

TABLE 4.

CALCULATED DATA FOR SUSPENSION RUNS

P_1 (psfa)	P_2 (psfa)	ΔP_{ft} (psf)	ΔP_{fa} (psf)	ΔP_{fp} (psf)	$(\Delta P_{ft})_{calc.}$ (psf)	α	$\alpha - 1$	T_m (^oR)	ρ_a (lb/ft^3)	Run & Tube No.
2,399	2,058	321	235	86	252	1.367	0.367	531.2	0.0789	52 D
2,752	2,082	670	575	95	567	1.166	0.166	531.9	0.0853	53 D
3,125	2,142	983	892	91	864	1.102	0.102	537.3	0.0919	54 D
2,418	2,096	322	258	64	259	1.249	0.249	539.4	0.0786	55 D
2,771	2,180	591	459	132	537	1.287	0.287	539.8	0.0862	56 D
3,125	2,115	1,010	931	79	941	1.086	0.086	539.9	0.0912	57 D
2,418	2,085	333	269	64	266	1.239	0.239	540.6	0.0783	58 D
2,771	2,120	651	585	66	578	1.112	0.112	540.8	0.0851	59 D
3,125	2,113	1,012	912	100	904	1.110	0.110	541.1	0.0909	60 D
2,418	2,111	307	232	75	237	1.323	0.323	541.2	0.0787	61 D
2,771	2,097	674	542	132	534	1.244	0.244	541.4	0.0844	62 D
3,125	2,120	1,005	803	202	777	1.250	0.250	541.5	0.0910	63 D
2,100	2,066	34	31	3	31	1.096	0.096	539.2	0.0724	64 C
2,136	2,067	69	62	7	62	1.113	0.113	538.8	0.0732	65 C
2,171	2,067	104	80	24	81	1.300	0.300	538.3	0.0738	66 C
2,207	2,068	139	118	21	116	1.178	0.178	538.2	0.0744	67 C
2,277	2,068	209	160	49	157	1.306	0.306	537.7	0.0759	68 C
2,348	2,068	280	189	91	181	1.483	0.483	537.5	0.0772	69 C

TABLE 5.

CALCULATED DATA FOR SUSPENSION RUNS

ρ_m $\left(\frac{lb}{ft^3}\right)$	$Q_a x10^4$ $\left(\frac{ft^3}{sec}\right)$	G_a $\left(\frac{lb}{ft^2 sec}\right)$	$G_p x10^2$ $\left(\frac{lb}{ft^2 sec}\right)$	R $x10^3$	u_a $\left(\frac{ft}{sec}\right)$	$(Re)_a$ $x10^{-2}$	$(Re)_m$ $x10^{-2}$	f_a $x10^3$	f_A $x10^3$	Run & Tube Nos.
0.0839	7.69	7.72	5.70	7.38	92.6	21.2	21.35	12.20	12.49	31 B
0.0962	9.13	11.08	6.96	6.28	115.8	28.9	29.08	11.18	13.93	32 B
0.1085	10.68	14.60	11.52	7.88	135.5	38.0	38.30	10.35	13.50	33 B
0.0846	5.85	6.18	9.28	15.00	74.2	16.1	16.37	9.93	19.17	34 B
0.0966	8.16	9.90	10.62	10.72	103.5	25.8	26.05	11.53	17.33	35 B
0.1088	9.25	12.65	11.94	9.44	117.3	32.9	33.20	10.78	17.98	36 B
0.0792	10.67	5.68	5.53	9.73	72.3	20.5	20.70	7.80	14.61	37 C
0.0856	24.26	13.97	12.69	9.08	164.6	50.6	51.10	9.70	5.22	38 C
0.0922	18.11	11.21	11.94	10.66	122.8	41.7	42.10	10.10	13.08	39 C
0.0984	22.30	14.77	10.37	7.03	151.2	53.5	53.80	9.45	10.72	40 C
0.1050	24.23	17.16	11.39	6.64	164.4	62.2	62.60	9.03	10.48	41 C
0.1118	25.95	19.53	9.83	5.03	175.9	70.7	71.10	8.75	10.22	42 C
0.0851	19.27	11.03	6.59	5.97	130.6	39.6	39.80	10.25	8.02	43 C
0.0988	20.25	13.68	15.08	11.02	140.1	49.0	49.50	9.65	11.92	44 C
0.1109	27.44	20.50	11.83	5.77	186.1	73.6	74.00	8.65	9.27	45 C
0.0857	14.14	8.09	12.90	15.93	95.8	29.0	29.45	11.15	14.80	46 C
0.0985	21.10	13.96	13.07	9.36	143.1	50.1	50.50	9.60	11.58	47 C
0.1096	26.87	19.87	9.82	4.94	182.2	71.3	71.70	8.73	10.06	48 C
0.0850	14.01	7.98	8.78	10.88	94.9	28.6	28.90	11.20	15.78	49 C
0.0989	19.98	13.22	17.32	13.10	135.6	47.4	48.00	9.75	13.27	50 C
0.1111	24.07	17.88	24.40	13.65	163.3	64.1	65.00	9.00	12.21	51 C

TABLE 5.

CALCULATED DATA FOR SUSPENSION RUNS

ρ_m $\left(\frac{lb}{ft^3}\right)$	$Q_a x10^4$ $\left(\frac{ft^3}{sec}\right)$	G_a $\left(\frac{lb}{ft^2 sec}\right)$	$G_p x10^2$ $\left(\frac{lb}{ft^2 sec}\right)$	R $x10^3$	u_a $\left(\frac{ft}{sec}\right)$	$(Re)_a$ $x10^{-2}$	$(Re)_m$ $x10^{-2}$	f_a $x10^3$	f_A $x10^3$	Run & Tube Nos.
0.0794	32.80	7.26	4.76	6.55	92.0	40.9	41.20	10.15	12.96	52 D
0.0856	50.80	12.17	3.09	2.54	142.7	68.6	68.80	8.83	10.43	53 D
0.0923	62.80	16.20	8.67	5.35	176.3	90.3	90.80	8.18	9.29	54 D
0.0796	33.15	7.31	8.64	11.82	93.0	40.4	40.80	1.02	1.27	55 D
0.0869	48.70	11.77	11.57	9.83	136.6	65.2	65.70	8.98	9.87	56 D
0.0920	65.80	16.83	14.81	8.79	184.7	93.2	93.90	8.13	8.72	57 D
0.0788	33.80	7.43	5.39	7.27	94.8	41.1	41.30	10.15	12.71	58 D
0.0856	51.20	12.22	6.67	5.45	143.7	67.7	68.10	8.85	9.97	59 D
0.0921	64.30	16.40	21.10	12.89	180.4	90.9	92.10	8.18	9.16	60 D
0.0809	30.74	6.79	19.07	28.10	86.3	37.6	38.60	10.65	13.82	61 D
0.0857	48.90	11.59	18.14	15.67	137.2	64.2	65.20	8.98	11.32	62 D
0.0923	57.80	14.77	22.10	14.96	162.3	81.7	82.80	8.68	11.21	63 D
0.0725	1.78	0.872	0.118	1.35	12.1	3.14	3.15	51.00	57.20	64 C
0.0733	3.57	1.770	0.206	1.17	24.2	6.38	6.40	25.05	28.05	65 C
0.0739	4.67	2.335	0.290	1.24	31.7	8.42	8.43	19.00	24.60	66 C
0.0745	6.69	3.375	0.337	1.00	45.3	12.15	1.22	13.18	15.71	67 C
0.0760	9.07	4.67	0.304	0.65	61.5	16.80	1.68	9.53	12.71	68 C
0.0772	10.48	5.48	0.269	0.49	71.0	19.72	1.97	8.10	12.49	69 C

TABLE 6.

CALCULATED DATA FOR SUSPENSION RUNS

f_C x10^3	$\frac{G_a G_p}{(G_a+G_p)^2}$	$\frac{(Re)_a G_a}{G_p}$ x10^{-5}	$\frac{\alpha-1}{R}$	$\frac{(Re)_a \rho_p}{\rho_a D_t^2}$ x10^{-10} (ft^{-2})	$\frac{(Re)_a \rho_p}{R \rho_a D_t}$ x10^{-11} (ft^{-1})	G_{mean} $\left(\frac{lb}{ft^2 sec}\right)$	$f_A (Re)_a^{0.2}$	Run & Tube Nos.
1.949	0.00729	2.87	X.X	35.8	1.537	7.77	0.0578	31 B
2.245	0.00622	4.60	31.35	42.6	2.145	11.14	0.0687	32 B
2.250	0.00778	4.82	29.33	49.7	1.995	14.71	0.0702	33 B
2.995	0.01456	1.08	55.5	27.3	0.576	6.27	0.0841	34 B
2.805	0.01050	2.41	37.9	38.0	1.123	10.00	0.0834	35 B
2.990	0.00927	3.49	52.5	43.1	1.440	12.78	0.0908	36 B
2.245	0.00955	2.11	84.2	19.6	0.876	5.73	0.0672	37 C
0.822	0.00892	5.57	X.X	44.8	2.140	14.10	0.0287	38 C
2.085	0.01042	3.91	22.43	34.4	0.605	11.32	0.0693	39 C
1.743	0.00694	7.61	15.38	41.2	2.540	14.87	0.0598	40 C
1.737	0.00657	9.37	18.82	44.8	2.920	17.27	0.0602	41 C
1.718	0.00498	14.06	25.23	47.9	4.120	19.62	0.0602	42 C
1.260	0.00591	6.63	X.X	35.2	2.560	11.09	0.0421	43 C
1.942	0.01078	4.44	17.6	37.9	1.485	13.82	0.0653	44 C
1.550	0.00571	12.77	88.5	50:3	3.772	20.62	0.0549	45 C
2.323	0.01547	1.82	18.7	25.8	0.703	8.22	0.0728	46 C
1.881	0.00920	5.35	17.85	38.6	1.786	14.09	0.0637	47 C
1.678	0.00489	14.43	22.26	49.2	4.320	19.95	0.0593	48 C
2.475	0.01064	2.63	33.3	25.6	1.023	8.07	0.0776	49 C
2.160	0.01287	3.62	21.52	36.5	1.210	13.41	0.0721	50 C
2.045	0.01328	4.69	19.71	44.0	1.398	18.13	0.0706	51 C

TABLE 6.

CALCULATED DATA FOR SUSPENSION RUNS

f_C $\times 10^3$	$\frac{G_a G_p}{(G_a+G_p)^2}$	$\frac{(Re)_a G_a}{G_p}$ $\times 10^{-5}$	$\frac{\alpha-1}{R}$	$\frac{(Re)_a \rho_p}{\rho_a D_t^2}$ $\times 10^{-10}$ (ft^{-2})	$\frac{(Re)_a \rho_p}{R \rho_a D_t}$ $\times 10^{-11}$ (ft^{-1})	G_{mean} $\left(\frac{lb}{ft^2 sec}\right)$	$f_A (Re)_a^{0.2}$	Run & Tube Nos.
1.991	0.00648	6.24	56.0	16.16	1.660	7.29	0.0684	52 D
1.638	0.002525	27.00	65.3	25.10	6.630	12.20	0.0613	53 D
1.486	0.00529	16.89	19.07	30.60	3.855	16.28	0.0575	54 D
1.944	0.01154	3.42	21.04	16.02	0.913	7.39	0.0668	55 D
1.558	0.00966	6.63	29.2	23.55	1.612	11.88	0.0572	56 D
1.393	0.00864	10.60	9.78	31.80	2.437	16.98	0.0542	57 D
1.952	0.00718	5.65	32.9	16.34	1.516	7.47	0.0672	58 D
1.568	0.00539	12.42	20.55	24.80	3.060	12.28	0.0581	59 D
1.463	0.01254	7.06	8.54	31.17	1.629	16.62	0.0567	60 D
2.135	0.02660	1.34	11.50	14.90	0.357	6.98	0.0716	61 D
1.781	0.01520	4.09	15.58	23.70	1.020	11.78	0.0654	62 D
1.790	0.01452	5.46	16.72	27.96	1.258	14.98	0.0680	63 D
8.570	0.001348	2.32	71.1	3.26	1.046	0.873	0.1802	64 C
4.240	0.001158	5.48	96.9	6.57	2.443	1.772	0.1022	65 C
3.740	0.001239	6.77	241.0	8.58	2.987	2.34	0.0945	66 C
2.385	0.000994	12.20	178.8	12.28	5.340	3.38	0.0652	67 C
1.936	0.000649	25.85	471.0	16.38	11.10	4.67	0.0562	68 C
1.909	0.000489	40.30	985.0	19.24	17.00	5.485	0.0568	69 C

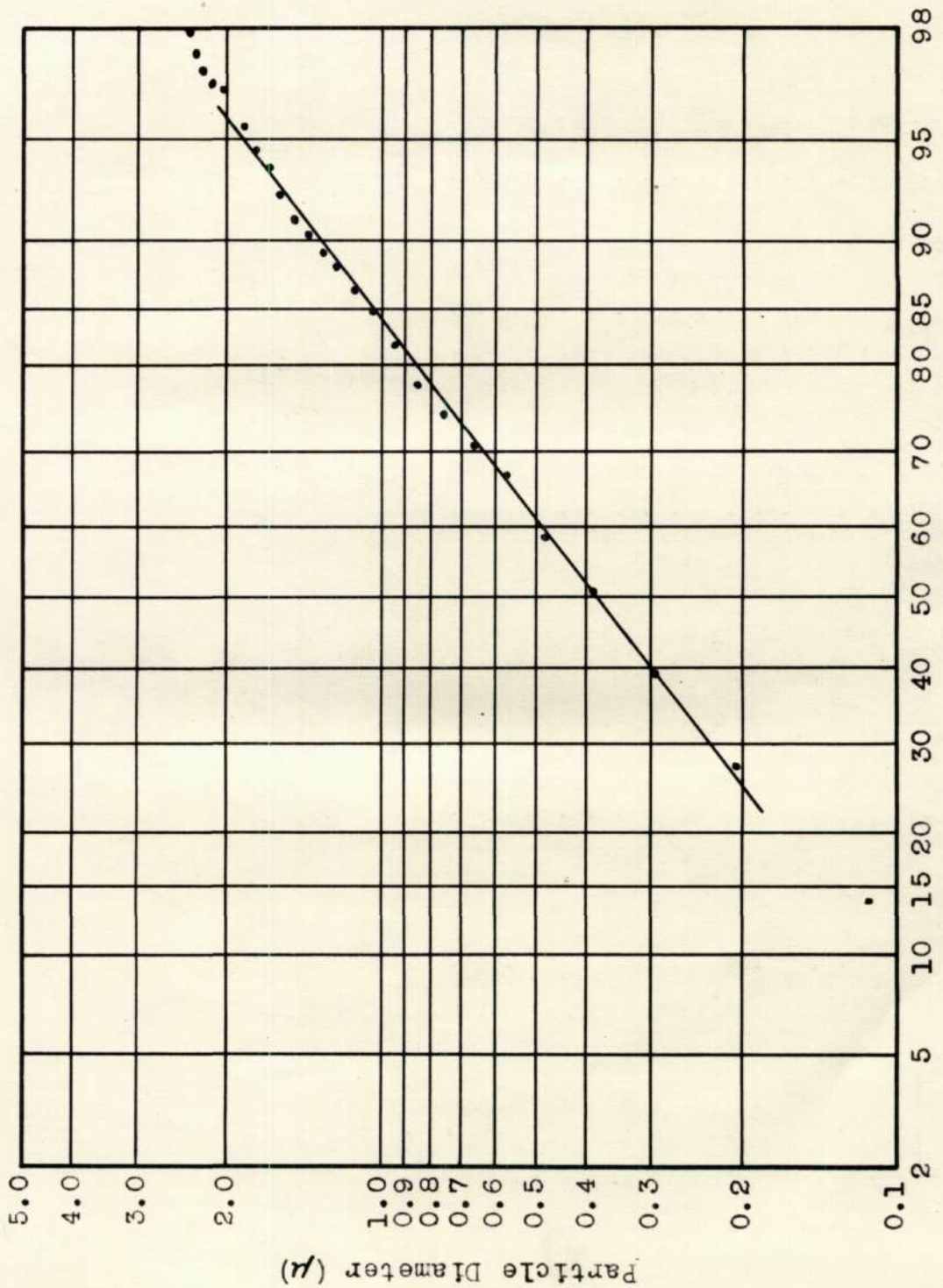

Fig. 14 Size Distribution of Powder

BIBLIOGRAPHY

1. Albright, C. W., Holden, J. H., Simons, H. P., and Schmidt, L. D., "Pressure Drop in Flow of Dense Coal-Air Mixtures." Ind. Eng. Chem. 43, 1837-40 (1951).

2. Belden, D. H. and Kassel, L. S., "Pressure Drops Encountered in Conveying Particles of Large Diameter in Vertical Transfer Lines." Ind. Eng. Chem. 41, 1174-8 (1949).

3. Chatley, H., "The Pumping of Granular Solids in Fluid Suspension." Engineering 149, 230-1 (1940).

4. Cramp, W., "Pneumatic Transport Plants." Chem. and Ind. 44, 207-11T, 211-13T (1925).

5. Culgan, J. M., "Pneumatic Conveying of Materials of Unit Density in a Three-Inch Pipe." Ph.D. Thesis in the School of Chemical Engineering, Georgia Institute of Technology, 1952.

6. DallaValle, J. M., Micromeritics. Pitman Publishing Company, New York, 1948.

7. Davis, H. F., "The Conveyance of Solid Particles by Fluid Suspension." Engineering 140, 1, 124 (1935).

8. Farbar, L., "Flow Characteristics of Solid-Gas Mixtures in a Horizontal and Vertical Circular Conduit." Ind. Eng. Chem. 41, 1184-91 (1949).

9. Gasterstadt, J., "Die Experimentelle Untersuchung des Pneumatischen Fordervorganges." Zeit. Vereinigung Deutschen Ingenieurw. 68, 617-24 (1924).

10. Hariu, O. H., and Molstad, M. C., "Pressure Drop in Vertical Tubes in Transport of Solids by Gases." Ind. Eng. Chem. 41, 1148-60 (1949).

11. Hinkle, B. L., "Acceleration of Particles and Pressure Drops Encountered in Horizontal Pneumatic Conveying." Ph.D. Thesis in the School of Chemical Engineering, Georgia Institute of Technology, 1953.

12. Jennings, M., "Pneumatic Conveying in Theory and Practice." Engineering 150, 361-3 (1940).

13. Korn, A. H., "How Solids Flow in Pneumatic Hardling Systems." Chem. Eng. 57, No. 3, 108-11 (1950).

14. Lapple, C. E., Alves, G. E., et al, Fluid and Particle Mechanics. University of Delaware, Newark, Delaware, 1951.

15. Perry, J. H., ed. Chemical Engineers Handbook. 3rd ed., McGraw Hill Book Co., Inc., New York, 1950.

16. Sadler, A. M., "Gas-Solids Fluidizing for Transport." Chem. Eng. 56, No. 5, 110 (1949).

17. Segler, G., "Untersuchungen an Kornergeblasen und Grundlagen fur die Berechnung." Zeit. Vereinigung Deutschen Ingenieurw. 79, 558-9 (1935).

18. Uspenskii, V. A., "Velocity of Particles and Coefficients of Resistance in Pneumatic Conveying." Za. Ekon. Topliva 8, No. 3, 26-30 (1951).

19. Vogt, E. G. and White, R. R., "Friction in the Flow of Suspensions: Granular Solids in Gases Through Pipe." Ind. Eng. Chem. 40, 1731-8 (1948).

20. Wagon, H., "Zur Bestimmung der Schwebegeschwindigkeit von Schuttgutern in Pneumatischen Forderanlagen." Zeit. Vereingung Deutschen Ingenieurw. 92, 577-80 (1950).

21. Wood, S. A. and Bailey, A., "The Horizontal Carriage of Granular Material by an Injection-Driven Air Stream." Proc. Inst. Mech. Engrs. (London) 142, 149-64 (1939).

22. Zenz, F. A., "Two Phase Fluid-Solid Flow." Ind. Eng. Chem. 41, 2801-6 (1949).